

UNIVERSITÀ
DEGLI STUDI
DI PADOVA

UNIVERSITA' DEGLI STUDI DI PADOVA

DIPARTIMENTO DI MEDICINA MOLECOLARE

SCUOLA DI DOTTORATO DI RICERCA IN

BIOMEDICINA

INDIRIZZO: Medicina Rigenerativa

CICLO XXVIII

Toll2 signalling safeguards Enteric Nervous System integrity

in *Drosophila melanogaster*

Direttore della Scuola : Ch.mo Prof. Stefano Piccolo

Coordinatore d'indirizzo: Ch.ma Prof.ssa Maria Teresa Conconi

Supervisore :Ch.mo Prof. Giacomo Carlo Sturniolo

Co-tutore: Ch.mo Prof. Ignazio Castagliuolo

Dottorando : Giulia Schirato

INDEX

SOMMARIO.....	5
1. SUMMARY.....	7
2.INTRODUCTION	9
1.1 Enteric Nervous System	9
1.2 Human neuropathies.....	10
1.4 Innate immunity.....	12
1.6 The <i>Drosophila melanogaster</i> model.....	16
1.7 The <i>Drosophila</i> gut	17
1.8 The Enteric Nervous System in <i>Drosophila</i>	18
1.9 Gut microbiota in <i>Drosophila</i>	19
1.10 <i>Drosophila</i> host defence	20
1.11 Innate immunity in <i>Drosophila</i>	20
1.12 The <i>Drosophila</i> Toll Signaling Pathway.....	22
1.13 <i>Drosophila</i> and intestinal inflammatory disease.....	24
1.14 Toll2 and Toll9.....	25
1.15 Construct the model <i>Drosophila</i>	25
3 AIM.....	27
4 MATERIALS AND METHODS	29
4.1 <i>Drosophila</i> Stock.....	29
4.2 Crossing with balancer	30
4.3 UAS GAL4 system	31
4.3a Temperature sensitive.....	32
4.3b Temperature inducible silencing.....	33
4.3b Chemically inducible	33
4.4 Life cycle and reproduction	34

4.5 Nutrient medium for <i>Drosophila melanogaster</i>	35
4.6 Bowel dissection	35
4.7 RNA extraction.....	35
4.8 RT-PCR	36
4.9 RealTime-PCR	37
4.10 Immunofluorescence	39
4.11 Survival analysis	39
4.12 Stress experiment with DSS	39
4.13 Analysis of global gene expression profile following toll silencing	40
4.14 Evaluation of the quality and integrity of the RNA extracted from the sample	40
4.15 Analysis of global gene expression profiling using microarrays	43
4.16 Analysis of data obtained from microarray	45
5 RESULTS	47
5.1 Efficiency of temperature sensitive GAL4 drivers	47
5.2 Reduced expression of different <i>toll</i> using ubiquitous driver actin	48
4.3 Ubiquitous <i>toll</i> silencing causes loss of intestinal neurons.....	48
5.4 Temperature inducible <i>toll</i> silencing.....	50
5.5 Cellular specific <i>toll</i> silencing causes loss of intestinal neurons.....	55
5.6 Increase survival in toll2 silenced.....	58
5.7 Increased survival of toll2-silenced flies following exposure to DSS.....	60
5.8 Analysis of microarray assay.....	62
5.9 Efficiency of chemically inducible GAL4 drivers.....	64
5.10 Silencing toll2 using the Gene Switch drivers reduced midgut neurons	64
5.11 Highlight decrease survival of toll2 silenced flies following exposure to DSS	68
6 DISCUSSION.....	69
7 BIBLIOGRAPHY	73

SOMMARIO

Studi scientifici e clinici hanno riconosciuto il microbiota intestinale come un organismo essenziale super-responsabile per il mantenimento della salute. Evidenze accumulate indicano che i cambiamenti nella composizione della comunità microbica intestinale sono coinvolti nella fisiopatologia di diverse malattie, tra cui malattia infiammatoria intestinale (IBD), anche se la popolazione cellulare e il meccanismo molecolare alla base sono ancora incerte. Il microorganismo intestinale interagisce con sensori microbici (ieTLR) in posizione strategica nella mucosa intestinale per generare una segnalazione cruciale nel preservare l'integrità della barriera epiteliale e omeostasi immunitaria locale. Pertanto, l'interruzione del microbiota intestinale e dei segnali derivati secondari di disbiosi o polimorfismi nei sensori microbici (es TLR2 e TLR4) può causare anomalie del sistema nervoso enterico, la rete neuronale distribuiti attraverso la parete intestinale. Poiché il SNE mantiene l'integrità della barriera epiteliale intestinale e l'omeostasi della mucosa immunitaria integrando diverse funzioni, il mancato conferimento dei giusti segnali dalla flora intestinale potrebbe predisporre a disturbi intestinali funzionali o infiammatori. Pertanto, questo progetto mira a identificare il meccanismo molecolare e cellulare dell'asse microbiota intestinale-immunità innata - SNE utilizzando l'organismo modello geneticamente trattabile *Drosophila melanogaster*. La *Drosophila melanogaster* è un modello ideale, perché è facile e poco costoso da mantenere, è eticamente ideale per questo progetto, tenendo conto l'elevato grado di conservazione da un punto di vista anatomico e dalle vie dell'immunità innata.

Per studiare il ruolo della segnalazione nell'integrità dell'SNE abbiamo usato il sistema UAS-GAL4 per indurre il silenziamento genico tessuto specifico. Così, abbiamo usato una linea driver che esprime la proteina GAL4 sotto il controllo ubiquitario (come tubulina o actina) o cellule specifico (elav per neuroni o mef per le cellule muscolari lisce) di un promotore con una linea UAS che porta un transgene specifico che in questo caso è una sequenza siRNA per toll. Il sistema GAL4 può essere temperatura e chimicamente (RU486) inducibile. In *Drosophila* con il toll2 silenziato in maniera ubiquitaria, temperatura inducibile, è stato rilevata una significativa perdita di neuroni HRP+. Inoltre, anche in *Drosophila* con silenziamento specifico del toll2 in cellule muscolari e cellule gliali abbiamo osservato una drammatica perdita di corpi neuronali HRP+. Le *Drosophila* con silenziamento delo toll2 sia ubiquitario che cellule specifico, hanno mostrato un aumento della sopravvivenza rispetto alla linea controllo w¹¹⁸. In presenza di una sostanza irritante gastrointestinale, destrano solfato di sodio (DSS), abbiamo osservato una ridotta sopravvivenza nei silenziati ubiquitari toll2, rispetto alla linea controllo w¹¹⁸.

Dal momento che la perdita di segnale toll2 sia a livello ubiquitario che cellule specifico ha causato una significativa perdita di neuroni, abbiamo effettuato una analisi del DNA espressione genica

microarray, nell'intestino di actina GAL4 UAS-toll2, elav GAL4 UAS-toll2, mef GAL4 UAS-toll2 e la linea di controllo w¹¹¹⁸, per identificare i geni a valle modulati dal segnale del toll2 coinvolti nello sviluppo neuronale e / o la sopravvivenza. Abbiamo identificato diversi geni coinvolti nelle vie notch, implicate nella formazione del sistema nervoso e nella differenziazione e sviluppo neuronale sostenendo ulteriormente l'opinione che i segnali toll2 di derivazione sono necessarie per supportare l'integrità neuronale enterica.

Per escludere effetti dipendenti della temperatura siamo passati al sistema UAS GAL4 chimicamente inducibile dalla molecola RU586. Utilizzando i driver ubiquitari abbiamo ottenuto un efficace silenziamento del toll2 in silenziati ubiquitari, associato a una significativa perdita di neuroni HRP +. Infatti, utilizzando driver cellulo specifici il silenziamento del toll2 è stato osservato nei mef GAL4 UAS-toll2 ma non negli elav GAL4 UAS-toll2. Di conseguenza, il silenziamento del toll2 è stato associato a una significativa perdita neuronale nella linea mef GAL4 UAS-toll2. Inoltre, il silenziamento ubiquitario toll2 utilizzando i driver GAL4 sensibili RU586 ha mostrato una drastica riduzione della sopravvivenza a seguito di esposizione DSS rispetto alla mosche di controllo w¹¹¹⁸.

In conclusione, utilizzando il modello di *Drosophila melanogaster* abbiamo dimostrato che i segnali toll2-derivati sono tenuti a sostenere l'integrità neuronale nell'intestino e cellule muscolari lisce sembrano più rilevanti fonti di segnali di sopravvivenza per i neuroni. Questi studi iniziali confermano la fattibilità di questo modello per studiare l'interazione innata immunità-nervi enterici e sezionare percorsi molecolari complessi relativi a patologie caratterizzate da una disfunzione dei nervi enterici.

1. SUMMARY

Scientific and clinical investigations have recognized the gut microbiota as an essential super organism responsible for maintaining health. Accumulating evidences indicate that changes in the composition of the gut microbial community are involved in the pathophysiology of several disorders including Inflammatory Bowel Disease (IBD), though the cellular population and the underlying molecular mechanism are still uncertain. Intestinal microorganism interact with microbial sensors (i.e.TLR) strategically located in the gut mucosa to generate signaling crucial in preserving epithelial barrier integrity and local immune homeostasis. Therefore, the disruption of gut-microbiota derived signals secondary to dysbiosis or polymorphisms in microbial sensors (i.e. TLR2 and TLR4) may cause anomalies in the enteric nervous system, the neuronal network distributed through the gut wall. Since ENS maintains intestinal epithelial barrier integrity and mucosal immune homeostasis by integrating different functions, failure to provide the right signals from the gut microbiota might predispose to intestinal functional or inflammatory disorders. Therefore, this project aim to identify the molecular and cellular mechanism of gut microbiota-innate immunity - ENS axis using the genetically-tractable model organism *Drosophila melanogaster*. The *Drosophila melanogaster* is an ideal model because is easy and inexpensive to maintain, is ethically ideal for this project taking into account the high degree of conservation from an anatomical point of view and from innate immunity pathways.

To study the role of toll signaling in the integrity of ENS we used the UAS-GAL4 system to induce tissue specific gene silencing. Thus, we have crossed a driver line which expresses the GAL4 protein under the control of ubiquitous (such as tubulin or actin) or cell specific (elav for neurons or mef for smooth muscle cells) promoters with a line UAS which carries a transgene that in this case is a specific siRNA sequence for toll. The GAL4 system can be temperature and chemically (RU486) inducible. In flies carrying ubiquitous, temperature inducible, toll2 silencing a significant loss of HRP⁺ neurons was detected. Moreover, also in flies with muscle cells and glia specific toll2 silencing we observed a dramatic loss of HRP⁺ neuronal bodies. Flies carrying both ubiquitous and cell specific toll2 silencing showed an increased survival as compared to w¹¹¹⁸ control flies. In presence of a gastrointestinal irritant, sodium dextran sulfate (DSS), we observed a reduced, as compare to control Wiii8, survival in flies carrying an ubiquitous toll2 silencing but not in flies with cell specific toll2 silencing.

Since loss of toll2 signaling following ubiquitous or cell specific silencing caused a significant loss of neurons, we performed a DNA microarray gene expression analysis, in the gut of act Gal4 UAS-toll2, elav Gal4 UAS-toll2, mef Gal4 UAS-toll2 and w¹¹¹⁸ control flies, to identify the downstream genes modulated by toll2 signaling involved in neuronal development and/or survival. We have

identified several genes involved in the notch pathways, implicated in the formation of nervous system as well as in neuronal differentiation and development further supporting the view that toll2-derived signals are required to support enteric neurons integrity.

To exclude temperature dependent effects we switched to UAS GAL4 system chemically inducible by the molecule RU586. By using ubiquitous drivers we obtained an effective toll2 silencing in act Gal4 UAS-toll2 flies associated to a significant loss of HRP⁺ neurons. Indeed, using cell specific drivers toll2 silencing was observed in mef Gal4 UAS-toll2 but not elav GAL4 UAS-toll2. Accordingly, toll2 silencing was associated to significant neuronal loss in mef Gal4 UAS-toll2 flies. Moreover, ubiquitous toll2 silencing using RU586 sensitive GAL4 drivers showed a dramatic reduction in survival following DSS exposure as compared to w¹¹¹⁸ control flies.

In conclusion, using the *Drosophila melanogaster* model we have shown that toll2-derived signals are required to support neuronal integrity in the gut and smooth muscle cells seem the most relevant sources of survival signals for neurons. These initial studies confirm the feasibility of this model to study the innate immunity- enteric nerves interplay to dissect complex molecular pathways relevant in pathologies characterized by a dysfunction of the enteric nerves.

2.INTRODUCTION

1.1 Enteric Nervous System

In vertebrates, the nervous system is organized in two large systems, the central and peripheral nervous system. The peripheral nervous system has in turn a division afferent and an efferent, the latter is formed by the somatic nervous system, which includes fibers of the motor neurons that innervate the skeletal muscles and the autonomic nervous system. The autonomic nervous system includes fibers that innervate smooth muscle cells, the cardiac muscle and glands. The peripheral nervous system is further divided into the sympathetic and parasympathetic systems which innervate most organs. The gastrointestinal has an wide intrinsic nervous system, termed the Enteric Nervous System (ENS) that can control functions of the intestine even when it is completely separated from the Central Nervous System (CNS) so is considered the "brain of the gut", controlling multiple functions of the intestine such as secretion of glands, mucosal absorption, blood flow, gut motility, and the activity of the mucosal(in particular immune system). But the ENS is not autonomous. In effect the control of gastrointestinal function by neurons is integrated structure connecting interactions between local enteric reflexes, that pass through sympathetic ganglia and reflexes that pass from the gut and through the CNS.

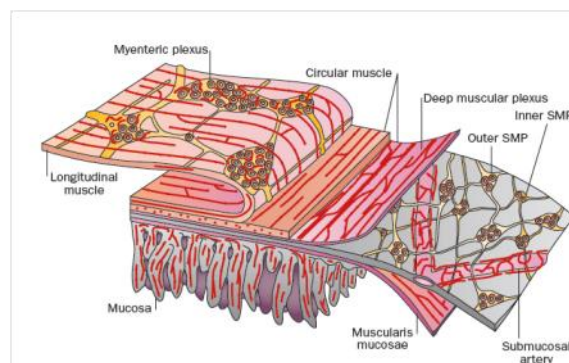


Figure 1 The organization of the ENS of human and mammals

The enteric nervous system (ENS) is divided into two main intrinsic plexuses, Meissner's plexus (submucosal), and Auerbach's plexus(myenteric), which are the two main networks of nerves that reside totally in the wall of the digestive tract from the esophagus to the rectum. It is composed of enteric ganglia, small aggregations of nerve cells, the neural connections and nerve fibers.

The ENS helps control both the process that regulates movement of fluid along epithelium and interacts with the endocrine and immune systems of the gut, both the process that maintains the integrity of the epithelial barrier inside the gut wall, it also regulates gastric secretion, determining the patterns of motility of the gastrointestinal tract, changing blood flow, modifying nutrient used.

(1)

1.2 Human neuropathies

There is a large range of neuropathies having as result one or more missed roles of the enteric nervous system. The term enteric neuropathy is reserved to the conditions with evident histopathology or depletion of enteric neurons. (2)

These neuropathies have been grouped as developmental or congenital; acquired and sporadic; associated with other disease states and iatrogenic or drug induced. Inflammation Bowel Disease (IBD) and Irritable Bowel Syndrome (IBS) are two common gastrointestinal disorders that present histopathological evidences of neuropathies. IBS is extremely common, affects up to 15% of the American population (3), IBD affect 800 subjects 1-1.3 million people in the same country (4). IBD are characterized by chronic intestinal inflammation and include Crohn's disease and ulcerative colitis, whereas IBS is characterized by physical symptoms, but there is no significant gut inflammation.

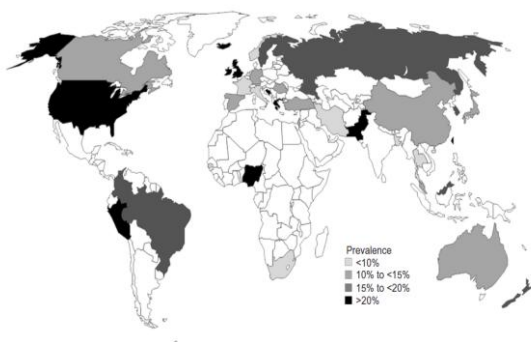


Figure 2 Worldwide prevalence of IBS

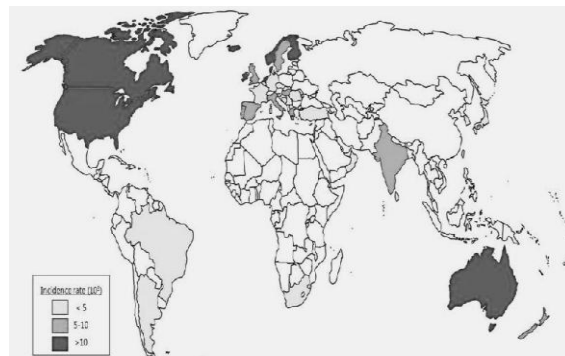


Figure 3 Worldwide prevalence of IBD

1.3 Intestinal microbiota

The gut microbiome comprises the collective genome of roughly 10^{14} microorganisms residing in the gastrointestinal tract. The gene repertoire of our gut bacteria contains 150 times more unique genes than the human genome(5). The relationship between the microbiota and the host is symbiotic, in fact, the host provides power and a sort of controlled microenvironment to intestinal bacteria, which in turn are beneficial to the host by improving the resistance to infection and facilitating 'absorption of ingested food. In metabolic terms, in fact, the microflora positively influences the permeability of the intestinal epithelium to facilitate the absorption of minerals and nutrients. The intestine is a particularly rich and diverse microbial habitat, in fact, about 800-1000

different bacterial species and more than 7000 different strains inhabit the gastrointestinal tract. The large intestine is densely populated as compared to the small intestine and also the microbial population associated with the mucosal layer differs from those present in the intestinal lumen. The microorganisms of the genus Bacteroides and Firmicutes are usually found in the small intestine and Bifidobacterium, Bacteriodes, Fusobacterium, Ruminococcus, Eubacterium, and Clostridium dominate in the large intestine. Although there is a wide variety in the intestinal microbiota and there is an inter-individual variability in the composition, it has been suggested that the microbiota in the majority of individuals can be classified into one of three variants or "enterotypes" that are common among individuals: Bacteriodes, Prevotella, and Ruminococcus. Molecular analysis revealed that the composition of the human intestinal microbiota is specific to each individual and relatively stable over time once each individual reach the age of maturity. The gut microbiome, in fact, undergoes a dynamic change during development, showing the most significant changes during childhood and adolescence. It is believed that the diversity of microorganisms and the change observed in this period are important for the functional development of the immune system and its impact on the health of future life. The microbiota has an important protective role, either by stimulating immunity and host defenses, that by modulating the proliferation and differentiation of intestinal epithelial cells by ensuring the barrier function. In particular, the intestinal microbiota plays a central role in the development and differentiation of the host immune system as demonstrated by hypoplasia of the lymphoid organs in mice germ-free. In addition, the commensal organisms of the gastrointestinal tract form a natural barrier that prevents the entry of pathogens, protecting the intestinal mucosa. Furthermore, the intestinal bacteria coming in contact with the epithelial cells are able to modulate the expression of molecules pro-and anti-inflammatory interacting with various components of innate immunity including Toll-like receptors. Under normal conditions in the intestinal microbiota prevail bacteria capable of reducing the expression of pro-inflammatory factors by reducing the reactivity of the immune-competent cells to the myriad of luminal bacteria. This delicate balance between microbiota and host, however, can be altered by changes in intestinal bacteria caused by diet or taking medications such as antimicrobials that determine significant and long-lasting changes in the structure of the commensal microbial flora. The decrease in colonization by members of the commensal microbiota leading to the expansion of antibiotic resistant strains and potentially pathogenic. Viral and bacterial infections or allergies can be favored by the changes in the microbiota induced by the use of antibiotics(6). It was also observed that following discontinuation of antibiotic treatment microbiota is not restored immediately in full, but the alterations persist

even in the long term. Antibiotics, therefore, changing the composition of the microbiota, which in turn influences the activity of the immune system can cause significant problems for the patient.

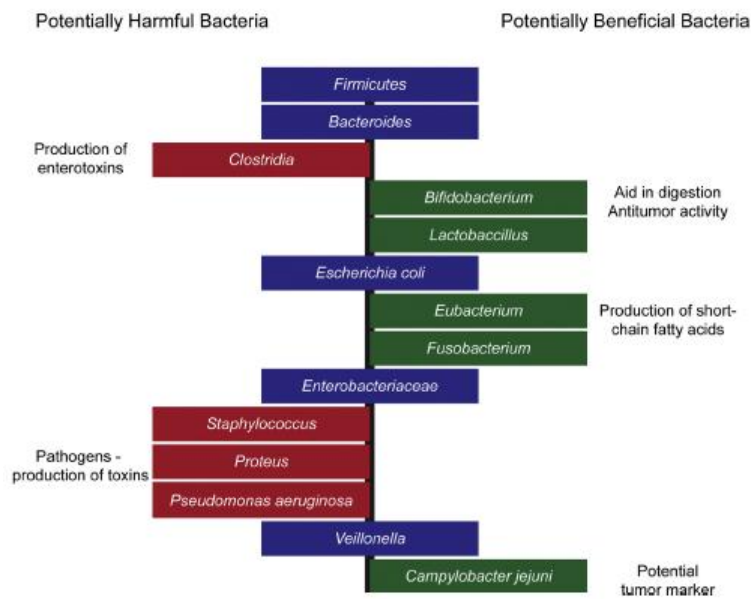


Figure4 Representation of potentially harmful and potentially beneficial bacteria present in the gut microbiome.

1.4 Innate immunity

There is a symbiosis between the mucosal innate immune system and endogenous microflora that favours a reciprocal growth, survival and inflammatory control of the intestinal network.

Immunity is organism's defense against pathogens or against components of the organism that no longer carry out their functions properly (for example, transformed cells). The immune system is basically divided into innate and adaptive immunity. A typical features of innate immunity are 1) the activity in a few minutes by infection with stereotyped responses, unlike the adaptive immunity that react later although generating more specific and robust responses 2)the ability of distinguishing between potentially pathogenic microbial components and not dangerous antigens by a set of cells and molecular pathways conserved during evolution that offers the first line of response in the occasion of exposure to microbes: pattern recognition receptors (PRRs) and among those toll-like receptors (TLRs) enable mammalian cells to recognize conserved characteristic molecules present on microorganism and described as pathogen-associated molecular patterns (PAMPs). TLR are transmembrane receptors that are present on phagocytic cells, dendritic cells, natural killer cells and other cells belonging to innate immune system. Modulating TLRs expression on immunosensory cells surface, microbiota can regulate the

intestinal innate immune system; recognition of microbes leads to activation of nuclear factor kappa B (NF- κ B) signaling pathway and consequently triggers cytokine production, up-regulation of co-stimulatory molecules on antigen presenting cells, leading to activation of T cells. Cells of innate immunity are able to produce cytokines essential for inflammatory reactions as well as factors critical for the subsequent initiation of specific immunity. The contact with bacteria and their components through the PRRs on their surface initiates innate immunity responses.

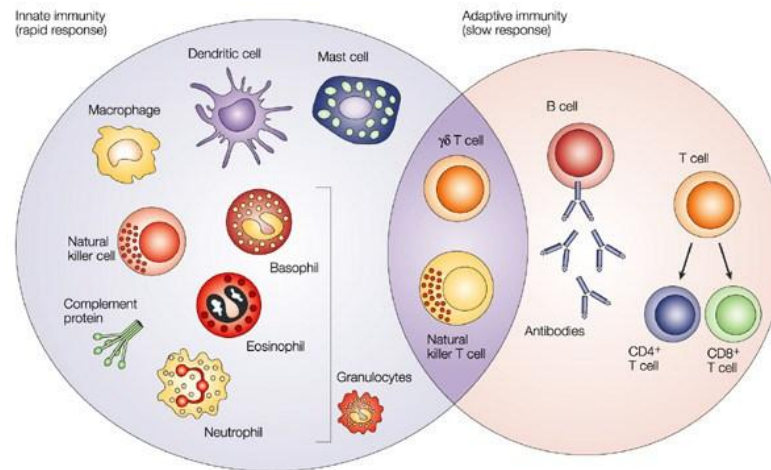


Figure 5 Immune system in mammals (8)

Then we can say that the expression and modulation of TLRs on intestinal epithelial cells and on dendritic cells (which represent the link between innate and adaptive immunity) have an active part during interaction with outside environment and in adaptation of the mucosal immune responses.

The major components of the adaptive response, located in the gut, is lamina propria where over a large number of macrophages, there are lymphocytes which once met the antigen produce antibodies. This type of response allows the body to increase the defensive capabilities in subsequent infections.

The innate and adaptive immunity cooperate, in particular thanks to the dendritic cells that result to be joining link between them, infact the innate responses provide proper signals to establish more powerful adaptive responses. (7)

1.5 Toll Like Receptor signaling

A class of receptors that plays a key role in the modulation of the immune response to gastrointestinal are Toll-Like Receptor. They are present on the wall of the epithelial cells and are capable of distinguishing molecular determinants specific, conserved during evolution, of microbial origin (PAMPs). Once recognized determinants bacterial, TLRs induce the activation of genes capable of triggering responses to control the infectious process. In particular characteristic structures of the bacterial cell such as lipopolysaccharides, lipoproteins, peptidoglycan that are not present in eukaryotic cells. TLRs are a family of transmembrane receptors characterized by an extracellular portion rich in leucine and an intracellular domain (TIR domain) which is a functional also present in other proteins of signal transduction. In mammals there are at least ten TLR, each recognizing different bacterial structure.

TLR2 is expressed in immune cells of the bowel, but also on enteric neurons, smooth muscle cells and glia. TLR2 deficient mice show complex anomalies in the ENS structure and neurochemical coding causing significant gut functional anomalies, including intestinal dysmotility and altered mucosal permeability. ENS anomalies were corrected by administration of glial cell line-derived neurotrophic factor (GDNF). Furthermore, in TLR2 deficient mice the increased colitis severity was abrogated following treatment with GDNF (9). Notably, wild type mice depleted of intestinal microbiota had similar defects in the ENS and intestinal motility as compared to mice deficient in TLR2. Moreover, we have shown that TLR2-derived signaling in smooth muscle cells is required to induce GDNF secretion, that in turn preserves enteric nerves integrity (REF). Although, it is not clear the contribute of other cell populations expressing TLR2 in maintaining ENS integrity.

TLR4 It was the first to be discovered and is expressed mainly by cells of the immune system, including macrophages and dendritic cells and is involved in the LPS signal. TLR4-mediated stimulation with LPS promoted enteric neuronal survival and supporting a role of intestinal microbiota in regulating gastrointestinal motility. (11)

TLR9 is located in the intracellular compartment of endosomes and is implicated in the recognition of particular regions of bacterial DNA with cytosines not methylated, CpG, which indicate the unequivocal presence of nucleic acids of bacterial origin. (12)

In general TLR signaling, regardless of the stimulated receptor, results in the activation of NF- κ B and MAP kinases to elicit regulatory responses. TLR3 and TLR7/TLR8 can also mediate the activation of IRF3 and IRF7 to trigger IFN induction. The signaling events initiated by TLR activation are mediated by unique interaction between TIR domain-containing cytosolic adapters, including myeloid differentiation primary-response protein-88 (MyD88), TIR domain-containing

adapter protein (TIRAP), TIR domain-containing adapter-inducing IFN β (TRIF), and TRIF-related adapter molecule (TRAM) (10). MyD88 serves as the central adapter protein associating with and thereby IRAK4 which in turn recruits and phosphorylates IRAK1. Following interaction with TRAF6, the activated IRAK complex phosphorylates TAB1 and TAK1, which in turn activate the NF- κ B and MAPK pathways. TLR3 functions through a MyD88-independent pathway by interacting with TRIF, thereby activating a complex of IKKe, TRAF3, and TBK1 that phosphorylates IRF3 and IRF7. Activation of IRF3 results in the induction of genes (such as CD40, CD80, and CD86) that stimulate T cell immunogenic responses. IRF7 promotes an antiviral immune response by the induction of IFN α and IFN β gene expression, whereas AP-1 and NF- κ B mediate inflammatory responses through the expression of interleukins (IL-1 β , IL-6, IL-8, and IL-12), macrophage inflammatory proteins, (MIP-1 α and MIP1 β), and cytokines (RANTES and TNF α). (13)

1.6 The *Drosophila melanogaster* model

Drosophila melanogaster, the common fruit fly, is an insect of the order of Diptera (from the greek di=two, and ptera=wings). Their body is about 2.5mm long, divided in three segments: head, thorax and abdomen; and have red eyes. In 1933 Professor Thomas Hunt Morgan won the Nobel Prize in Physiology and Medicine for showing that genes are carried on chromosomes and are the basis of heredity, using as a model *Drosophila melanogaster*.

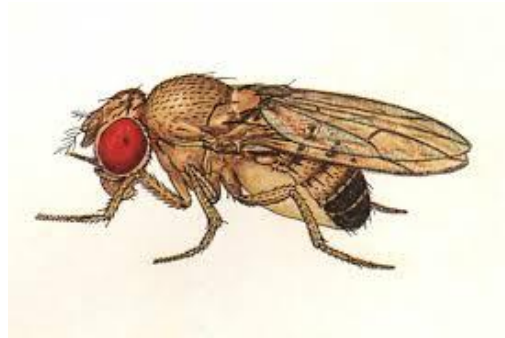


Figure 6 *Drosophila melanogaster*

Today is one of the most successfully used and most versatile genetic model organism.

An ideal model system should reflect the human biology, while reducing the complexity of the human disease of interest, such that it can be studied and manipulating effectively.

Drosophila has many advantages for biochemical studies. Flies are readily available from stock center and are easy and inexpensive to maintain and, as invertebrates, flies are ethically ideal for research purposes(14). Also *drosophila* has a rapid generation time, quickly producing an abundant progeny. From a genetic point of view, *Drosophila* has a compact genome with low redundancy. As compared to mammalian genome, *Drosophila* genome contains fewer paralogs of intestinal regeneration-controlling genes and a simple cellular structure. Moreover, in *Drosophila* are easily available a number of sophisticated genetic tools that are superior to other model animals including RNAi and UAS-GAL System that will be explained below.(15)

But more importantly for our project *Drosophila* can be used as a model of human intestinal infection and pathology, since several intestinal regeneration and signaling pathways are conserved between *Drosophila* and mammals.

1.7 The *Drosophila* gut

Fly and human intestines have in common tissue anatomy and physiological functions. The *Drosophila* gut consists of a simple epithelium, enclosed by nerves, visceral muscles and tracheae. Depending on their position along the length of the gut, the nature and arrangement of these different cell types differ. For example in the digestive epithelium, which is subdivided into foregut, midgut, and hindgut, depending on the height at which they are located along the digestive tract. (17)

The *Drosophila's* foregut corresponds to the mammalian's esophagus, the crop to the stomach, the midgut to the small intestine and hindgut-rectum-anus to the large intestine-rectum-anus (15). The foregut and hindgut epithelium are of ectodermal origin and are smooth by an impermeable cuticle. In contrast, the midgut epithelium is of endoderm origin and is protected on the luminal side by the peritrophic matrix. The adult midgut is additionally divided into six main anatomical regions with digestive functions and different metabolic activities. Some of them are delimited by anatomically distinct sets of muscles, suggesting a sphincter-like role in regulating the motility. Thorough genetic and histological analyses have revealed additional regionalization of these midgut regions. This regionalization seems to be a common property of the *Drosophila* digestive tract because it has also been observed in the proventriculus and larval midgut and hindgut. It is notable that the organization of larvae and adults digestive tract differs from a genetic and anatomical point of view, probably because a result of their different dietary habits.

While larvae feed incessantly to maintain their growth and are able to ingest solid food thanks to their mouth hooks, adult flies feed less frequently, ingesting liquid via their proboscis. This alternating ingestion of liquid may account for the presence of the crop, a storage organ found only in adults. (17)

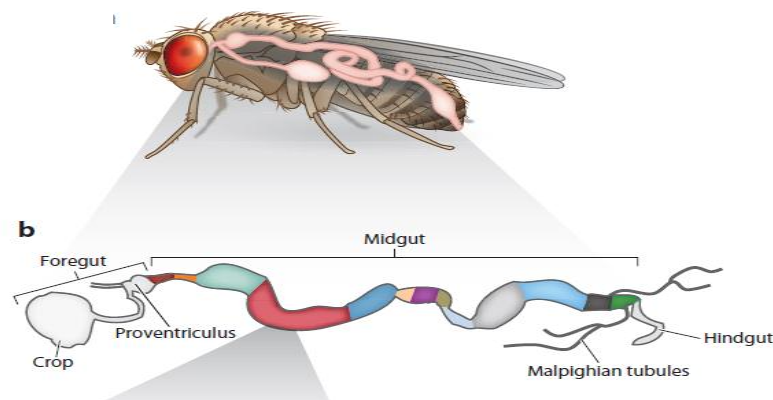


Figure7 The digestive tract is divided into three discrete domains of different developmental origin: foregut, midgut, and hindgut. Each of these domains is further subdivided into genetically distinct compartments

The adult *Drosophila* gut is divided in three distinct gastrointestinal tissue, corresponding to the stages development, that during development replacing one another: the larval gut, the pupal gut, and the adult gut. The adult midgut epithelium contains two types of differentiated cells: enterocytes and enteroendocrine cells (EECs). Enterocytes (also called columnar cells in other insects) are large polyploid cells that absorb nutrients, secrete digestive enzymes and differ distinctly in morphology along the gut. As in other insects the adult midgut is constantly replaced by new cells derived from intestinal stem cells (ISCs) spotted across the basal surface of the gut epithelium. Midgut ISCs divide asymmetrically or symmetrically. In asymmetric divisions, one daughter cell maintains ISC characteristics and remains mitotic, while the other daughter cell exits the cell cycle and differentiates into either an absorptive enterocyte or an EEC, a consequence determined by Notch signaling activity. All midgut ISCs and enteroblasts (referred to together as progenitor cells) express the marker gene *escargot*. But, distinct populations of self-renewing stem cells have been identified along the digestive tract. Also, in the foregut-midgut junction another subpopulation of self-renewing cells is found. In the hindgut, stem cells are limited to a thin segment known as the hindgut proliferation zone located at the midgut-hindgut boundary. The different stem cell populations may contribute to the organization of different regional identities. Alternatively, or in parallel, adjacent tissues, such as visceral muscles and tracheae, could provide region-specific position signals to differentiating ISC and to maintaining regional identity to their progeny.

The midgut epithelium is renewed within one to two weeks at the same conditions. Stem cell activity is inclined by environmental factors and the metabolic state of the host. In the fed condition, localized insulin signaling increases ISC activity and drives tissue growth. Improved stem cell activity is also observed upon intestinal damage by corrosive agents or pathogenic bacteria. This allows the rapid regeneration of the compromised gut and maintains barrier integrity. (17)

1.8 The Enteric Nervous System in *Drosophila*

The adult digestive tract in *Drosophila* is innervated in three distinct regions: the esophagus-crop-anterior midgut, the midgut-hindgut junction, and the posterior hindgut, that accept innervations from the stomatogastric nervous system, the corpus cardiacum, the hypocerebral ganglion and neurons located in the central nervous system (CNS), which extend their axons toward three sections of the digestive tract (foregut, midgut, hindgut).

The areas that have epithelium most innervated are the esophagus, pyloric valve, and rectal ampulla and have secretion and absorption properties.

Dendrites coming from peripheral sensory neurons are evident in the anterior- and posterior regions of the digestive tract, and they are showed most copious in the esophagus and anterior midgut, demonstrating that not all are efferent innervation. Few neurons are found in proximity to the digestive tract and they contribute to this sensory innervations. It would also seem that there are such big differences between larvae and adults, since serotonin positive neuronal fibers, ion transport peptide and some neuropeptides were found in both the larval and/or adult hindgut. It is notable that all three innervated regions receive insulinergic innervations. The two populations of insulin-producing neurons have synaptic links in the CNS, this suggests that they have a role in interconnected circuit to regulate the release of insulin to different part of the digestive tract. (17)

1.9 Gut microbiota in *Drosophila*

Drosophila feed on decaying fruit, and their digestive tract is so constantly exposed to food microbes, which may themselves contribute to digestion. The *Drosophila* gut lumen is an environment with relatively low bacterial diversity five OTUs (*Acetobacter pomorum*, *Acetobacter tropicalis*, *Lactobacillus brevis*, *Lactobacillus fructivorans*, and *Lactobacillus plantarum*). and numbers (1–30 species, 10³–10⁵ CFU/fly). Not yet been officially confirmed the present of a constant population of dividing bacteria residing in the gut, because bacteria found in the *Drosophila* gut are also found in the substratum, suggesting regular contamination (18). Experiments with germ-free flies (raised in the absence of both internal and external bacteria) have shown that gut-associated bacteria can be helpful to *Drosophila* by promoting growth in poor nutritional conditions. Unfortunately has yet to be recognized how bacteria contribute to development, but they aren't only a food source given that growth promotion was only observed in the presence of live bacteria (18). Bacteria in the foodstuff can modify its nutritional content, predigesting food, and/or improve digestion in the gut. Gut bacteria also stimulate intestinal epithelial turnover and control the basal level of antimicrobial peptide gene expression in the gut. Although less studied, turn out to be important even yeasts that play an significant role in *Drosophila* diet by given many essential nutrients not present in plant material: sterols, B vitamins, amino acids and fatty acids. (19)

1.10 *Drosophila* host defence

Drosophila represents an ideal model system in which to study host-pathogen interactions since insects have a particularly effective immune system that appears to be evolutionarily conserved. The first line against microorganism is body's epithelial surface. To inhibit microbial growth there is a production of antimicrobial peptides by the epidermis of the tracheae and of the Malpighian tubules. Microorganism that succeed to enter the general body cavity are attacked by both cellular and humoral defenses. The cellular defenses consist of phagocytosis by macrophage-like cells, called the plasmatocytes. Lamellocytes instead encapsulate larger invading microorganisms. The characteristic of the humoral reactions is the systemic antimicrobial response: produce synthesis of antimicrobial peptides by the fat body. The humoral reactions also involve several proteolytic cascades. The melanization cascade is very important because, generating quinones and toxic oxygen and culminating in the production of melanin at injury sites or around microorganisms, can encapsulate and sequester pathogens. Another cascade: the Hemolymph zymogen plays a crucial role in activating the synthesis of antimicrobial peptides in the fat body.(20)

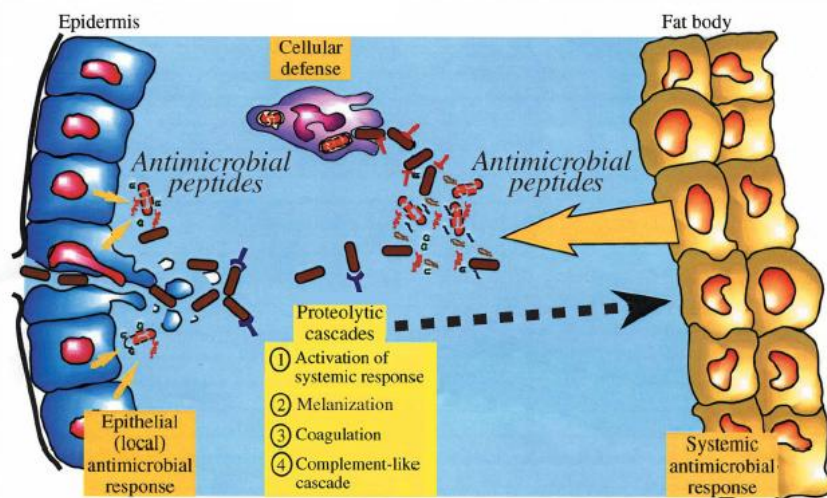


Figure 8 The antimicrobial defense of *Drosophila*

1.11 Innate immunity in *Drosophila*

In response to microbial challenge, *Drosophila* induces the expression of a variety of small peptides with potent antifungal and antibacterial activities. These peptides provide efficient host

protection because they directly kill invading microbes (Diptericin, Attacin, Drosocin, Cecropin, Defensin, Drosomicin). The promoters of the genes encoding these peptides contain sequence motifs related to mammalian NF- κ B response elements. Depending on the invading pathogen, *Drosophila* activates either the Imd- or Toll-signalling pathways, which in turn induce the expression of pathogen-specific sets of antimicrobial peptides. While fungal and bacterial infection stimulates the Toll pathway, the Imd pathway mediates only antibacterial responses. Activation of either Toll or Imd signalling results in the activation of distinct NF- κ B-like transcription factors. Similarly in mammals, members of the NF- κ B protein family play a central role in the regulation of inflammatory and innate immune responses. The conservation of the NF- κ B regulatory mechanisms between organisms as diverse as insects and mammals indicate that the regulation of the innate immune response is evolutionarily conserved. Recent evidence suggested that Toll signalling is required to fend off fungal and Gram-positive bacterial infection. In contrast, the Imd pathway appear required to protect *Drosophila* against Gram-negative bacterial infections. The observation that different pathogens trigger distinct signalling cascades led to the model whereby different classes of invading microbes may activate distinct members of the NF- κ B protein family.

-toll signal transduction pathway is activated in response to fungal and Gram-positive bacterial infections: toll activation results in the expression of a subset of genes encoding antimicrobial peptides. The Toll signal transduction cascade shares striking similarities to the TLR/NF- κ B pathway of mammals. The following *Drosophila* mammalian proteins share strong homologies: Toll/TLR, dMyd88/Myd88, Pelle/IRAK, Cactus/I- κ B and Dif,Dorsal/NF- κ B. However, unlike in the mammalian TLR/NF- κ B pathway, in *Drosophila* the Toll receptor is activated by the cytokine ligand Spätzle that is cleaved by proteases activated by circulating “Pattern Recognition Receptors” (PGRP-SA and GNBP-1 for Gram positive bacteria). (21)

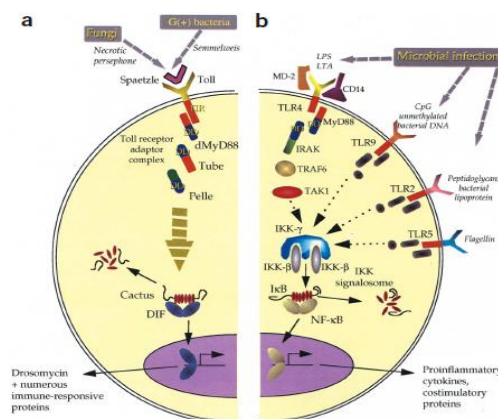


Figure9 Toll pathways in *Drosophila* and mammals

-Imd pathway is activated in response to Gram-negative bacterial infection: Imd activation causes the expression of antibacterial peptides. This pathway share similarities with the TNF-R1 pathway. The following *Drosophila*/mammalian proteins share homologies: Imd/RIP, dTAK1/MEKK3, dmIKKg/IKKg, dmIKKb/IKKb, Dredd/Caspase-8, and Relish/p105. Differential activation of the Toll or Imd pathway during bacterial infection is triggered through exposure to bacteria-specific peptidoglycans. The lysine-type peptidoglycan from Gram-positive bacteria is recognized by PGRP-SA and GNBP-1 and activates the Toll pathway while the meso-DAP peptidoglycan from Gram negative bacteria is recognized by PGRP-LC activating the Imd pathway.(22)

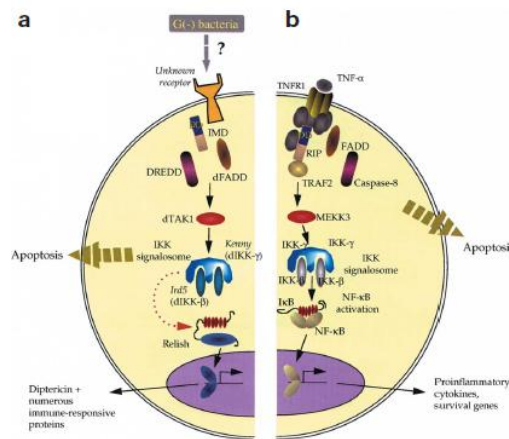


Figure10 The Imd pathway of *Drosophila* and the TNF- α receptor pathway in mammals

1.12 The *Drosophila* Toll Signaling Pathway

Toll is a transmembrane receptor first identified as an essential component in dorsal-ventral embryonic development in *drosophila*. If are Gram positive bacterial peptidoglycan to stimulate toll pathway, it is used like mediators the extracellular peptidoglycan recognition protein (PGRP)-SA. There are twelve genes, in addition to splice isoforms, coding for the many PGRPs in *Drosophila*. The PGRPs are grouped into Short class (such as -SA, -SB, -SC, -SD) and the Long class (such as -LA, -LB, -LC, -LD, -LE). Another recognized pattern-recognition is a protein called Gram-negative binding protein-1 (GNBP-1), that is also required for upstream recognition of Gram-positive bacteria 16 and 21. High-level expression of PGRP-SA and GNBP-1 simultaneously, but not individually, leads to constitutive activation of the Toll pathway (23). Gram-positive bacteria-associated molecules are recognized by multiple host proteins, which then work together to stimulate the Toll pathway. The stimulation of the Toll pathway by fungi, instead,

involves a serine protease, Persephone, and a protease inhibitor, Necrotic; doesn't depend on PGRP-SA or GNBP-1. Instead during embryonic development it is a serine protease cascade that regulates Toll, then has different proteases from those in the immune response. Spätzle guides the upstream regulatory cascades in dorsal-ventral patterning of the Gram-positive bacterial response and the fungal response. Recent experiments show that Spätzle probably acts as a ligand for Toll, activating the Toll pathway. Toll activation involves receptor multimerization. It has been demonstrated that multimerization of Toll increases signaling activity, using various chimeric and mutant constructs. Activation of Toll leads to employment of three cytoplasmic proteins: Tube, MyD88 and Pelle, to form the signaling complex below the cell membrane. MyD88 and Tube act as adaptor proteins and Pelle is a serine-threonine kinase. The TIR domain of MyD88 is conducted to the TIR [Toll-inter-leukin-1 (IL-1) receptor] domain of Toll binds, however, only when the receptor is active. Subsequently, through interactions of death domains, occurs assembly of the signaling complex containing MyD88, Tube and Pelle. The Pelle kinase activity is stimulated by improved local concentration of Pelle might lead to trans- phosphorylation. The activated Pelle acts on the cytoplasmic Dorsal-Cactus and Dif-Cactus complexes, but isn't yet defined manner. Dif and Dorsal are NF- κ B homologues and are normally preserved in the cytoplasm by the I κ B-related inhibitor Cactus. Dif and Dorsal are moved to the nucleus and activate the expression of antimicrobial peptide genes, after signal-induced degradation of Cactus.

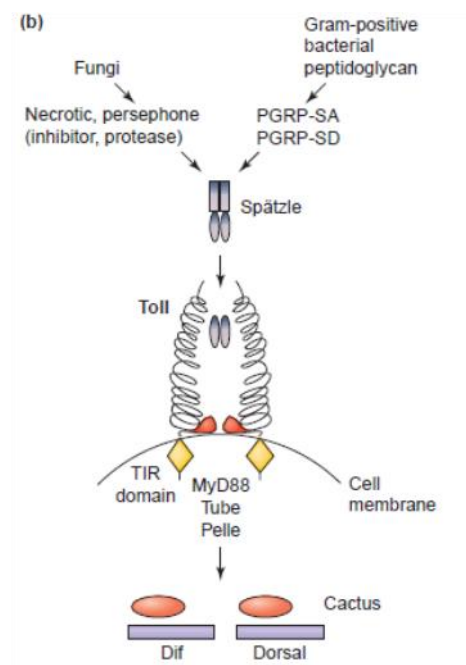


Figure 11 molecular cascades of Toll

1.13 *Drosophila* and intestinal inflammatory disease

The fruit fly *Drosophila melanogaster* is a useful model system in which to study mechanisms of intestinal homeostasis and disease, because it has numerous anatomical features that are similar to the human intestine. The intestinal epithelium of the fly contains proliferating and differentiated epithelial cells that are comparable to those of the vertebrate intestine, this is important to understand the factors that regulate IBD, because they have been shown to be associated with alterations in enterocyte proliferation. JAK-STAT pathway for example is one of several pathways that regulate intestinal stem cell signaling in flies that are also present in mouse and human enterocytes. In IBD, the intestinal epithelium suffers a marked loss of enterocytes through apoptosis, which conducts to defaults in the intestinal barrier that enables for the transmucosal passage of bacteria and activation of the host immune system. In the fly it was showed that JNK signaling plays key roles in regeneration of the fly intestine by directing the increase of intestinal stem cells in a process that requires Delta and Notch signaling (24). The activation of JNK in the intestine lead to a loss of enterocytes by apoptosis when flies were administered *Pseudomonas aeruginosa*, resulting in compensatory improved proliferation that was dependent upon the activation of the cell cycle regulatory protein Ras1. Indeed, by administering the epithelial toxins dextran sulfate sodium (DSS) and bleomycin to flies that were expressing proapoptotic proteins, it was demonstrated that the induction of enterocyte apoptosis itself might serve as a signal for the generation of mature enterocytes from precursors in the intestine (25). Similarly, in response to oxidative stress - which is known to play an important role in enterocyte apoptosis in IBD - epithelial cells in the fly undergo apoptosis that require the activation of cell-specific inositol - trisphosphate 3-kinase. The regulation of epithelial apoptosis in the fly requires two pathways connecting to IBD: the small GTPase Rho1 and its effects on JNK signaling. The fly has also been used to determine the pathways of regulation of mitogen-activated protein kinase (MAPK) signaling in the intestinal epithelium, also present in the mammals homeostasis.

The discovery more interesting for our work it was identification of the molecule Toll, which is implicated in antifungal responses and in the regulation of gut homeostasis by influencing the balance between stem cell repair and microbe-induced epithelial cell damage. In mammals, the first Toll-like receptor that was identified (TLR4) has been shown to identify endotoxin through MD2. Studies performed in mice TLR4 deficient or related genes have demonstrated the role of these innate immune receptors in the pathogenesis of IBD .

1.14 Toll2 and Toll9

In particular we decided to focus on two different tolls, connected to TLRs studied in mice by our group:

-*18-wheeler*: corresponding to TLR2, is an essential receptor for the *Drosophila* humoral immune response. It has been demonstrated that encodes a protein with receptor-like structure. It is expressed in the fat body at the appropriate time to be active in the larval antimicrobial response. *18w* mutant flies show increase lethality in the face of bacterial challenge. Consistent with its sequence similarity to the cytoplasmatic domain of type I IL-1Rs, *18w* plays a role in nuclear recruitment of the Rel factor Dif to the nucleus. *18w* is transcriptionally induced upon infection and in mutants were found alterations in antimicrobial gene expression following infection. A major reduction is seen in *attacin*, *cecropin*, *diptericin*. (26)

-*toll9*: corresponding to TLR9, activates strongly the expression of drosomycin, and utilized similar signaling components to toll-1 in activating the antifungal gene. The predicted protein sequence of toll-9 contains a tyrosine residue in place of a conserved cysteine, and this residue switch is critical for the high activity of toll-9. The toll-9 gene is expressed in adult and larval stages prior to microbial challenge, and the expression correlates with the high constitutive level of drosomycin mRNA in the animals, so it is a constitutively active protein, and implies its novel function in protecting the host by maintaining a substantial level of antimicrobial gene products to ward off the continuous challenge of microorganism. (27)

1.15 Construct the model *Drosophila*

The fruit fly can be used with two types of gene functional strategies "forward-genetics" and "reverse-genetics". The "forward-genetics" is an effective method to investigate a wide spectrum of biochemical processes. In flies it is possible to introduce mutations that are later selected on the basis of the phenotype they induce. In the "reverse genetics" it is identified in the fly the homologue of a gene involved in a human disease and the phenotype resulting from its altered expression is studied. These phenotypes are generated by reducing, eliminating or suppressing the homologue of the pathological gene in order to understand the function of its product protein (28). There are two methods used to examine a causative gene in *Drosophila*:

- **loss of function** of the homologous gene in the fly. This is possible by transposable elements that were going to destroy the gene of interest. The transposable elements are employed also to

generate transgenic individuals: the element P, that are used a vehicle for the insertion of an exogenous gene into the host genome. This technique allows you to generate several independent lines of transgenic flies for each construct of interest.

- **RNAi nterference (RNAi)** used to suppress the expression of an endogenous gene by a construct that expresses a hairpin RNA double filament able to suppress the translation into protein or degrade homologous mRNA in tissue specific manner or at a certain stage of development. thanks to the system expression binary UAS / GAL4, the transgene can be expressed in more tissue or in small groups of specific cells. Once the model of *Drosophila* has been developed, the resulting phenotype can be studied extensively going to determine the cellular or molecular level pathogenic process of interest. (28)

3 AIM

The working hypothesis behind this project was that the ENS neuropathy observed in several intestinal disorders is not purely a histopathological hallmark of chronic inflammation but may rather result from the anomalous signalling of the innate immunity system/gut microbiota thus contributing to the onset/severity of intestinal disease. To provide experimental support to our hypothesis we took advantage of the genetically-tractable model organism *Drosophila melanogaster* to:

1. determine the role of different toll-derived signals in preserving the integrity of the neurons in the intestinal tract in drosophila
2. identify the cell population(s) generating toll-derived signals supporting enteric neurons integrity.

4 MATERIALS AND METHODS

4.1 Drosophila Stock

UAS lines used are:

-toll1: P{KK103505}VIE-260B

-toll2: w[118]; P{GD 2513}v 44386/TM3; v 44387; v 36305

-toll4: P{KK103537}VIE-260B

-toll6: P{KK105856}VIE-260B

-toll7: w[1118]; P{GD16}v24473/TM3

-toll8: w[118]; P{GD 14437}v 27098/TM3; v27099

-toll9: P{KK101880}VIE-260B

GAL4 driver temperature:

-Actin-Gal4 driver line: y1 w^{*}; P{GAL4-Act5C 25FO1/CyO, y⁺}. Strain in which the sequence gal4 is controlled by the actin promoter, and is therefore expressed ubiquitously in all cells of the body.

-Tub-Gal4 driver line: y1 w^{*}; P{tubP-GAL4}LL7/TM3. Strain in which the sequence gal4 is controlled by the tubulin promoter, and is therefore expressed ubiquitously in all cells of the body.

-Elav-Gal4 driver line: P{w [+ mW.hs] = GawB} elav [C155]. In this strain the sequence gal4 was placed under the control of the promoter embryonic lethal abnormal vision (elav) gene expressed in the nervous system of Drosophila in a generalized way.

-Mef-Gal4 driver line: y1 w^{*}; P{GAL4-Mef2.R}3. Strain in which the sequence gal4 is controlled by myocyte enhancer factor (Mef) which is expressed in muscle cells.

-Repo-Gal4 driver line: w[1118]; P{w[+m^{*}]=GAL4}repo/TM3. In this strain the sequence gal4 is controlled by reverse polarity gene promoter, a target gene of glial cells.

GAL4 driver steroid dependent:

-Actin-Gal4 driver line: P{ry[+t7.2]=hsFLP}12, y[1] w[*]; P{w[+mC]=UAS GFP.S65T}Myo31DF[T2]; P{w[+mC]=Act5C(-FRT)GAL4.Switch.PR}3/TM6B, Tb[1]. Expresses a progesterone-inducible GAL4 in all cells.

-Elav-Gal4 driver line: y[1] w[*]; P{w[+mC]=elav-Switch.O}GSG301. Expresses steroid-activated GAL4 in neurons.

-Mef-Gal4 driver line: w[*]; P{w[+mW.hs]=Switch2}CG2765[GSG8708]/CyO. Expresses steroid-activated GAL4 in muscles.

-Repo-Gal4 driver line: y[1] w[*]; P{w[+mW.hs]=Switch2}GSG1201-2. Expresses steroid-activated GAL4 in CNS and PNS glia.

-Arm-Gal4 driver line:w[*]; P{w[+mW.hs]=GAL4-arm.S}1. Expresses GAL4 in arm[+] pattern.

Balancer lines:

-CyO: *curly*, morphological marker of the second chromosome which produces a phenotype "wings curled up" and is lethal in homozygosity.

-TM3/TM6: *stubble*, morphological marker of the third chromosome balancer, which produces phenotype "bristles short and thick" and is lethal in homozygosity.

4.2 Crossing with balancer

Insertion in chromosome II

P: ♀ (o ♂) transgenico w+ x ♂ (o ♀) Sm6a (CyO)/Tft

By midges born in the F1 generation we choose individuals with phenotype w + (red eye, for the presence of the transgene) and CyO (*curly*, morphological marker of the second chromosome which produces a phenotype "wings curled up" and is lethal in homozygosity), which are crossed between them. If the insertion of the transgene has taken place in the

second chromosome, all the individuals of F2 generation have w + phenotype, i.e. have red eyes because the allele *Sm6a* is homozygous lethal. Otherwise, if the phenotype also appears "White eye", it means that the insert is incorporated into another chromosome.

Insertion in chromosome III

P: ♀ (♂) transgenico w+ x ♂ (♀) TM3 (Sb)/TM6

In the F1 generation we choose individuals with phenotype w + (red eye) and Sb, (stubble, morphological marker of the third chromosome balancer, which produces phenotype "bristles short and thick" and is lethal in homozygosity), which are crossed each other. If the transgene is inserted into chromosome III, all individuals of the F2 present the w + phenotype because the Sb allele is homozygous lethal. On the contrary, indicates that the insert is integrated in another chromosome.

4.3 UAS GAL4 system

The GAL4/UAS system is a biochemical method use to study gene expression and function in fruity fly. In the UAS-GAL4 system, there are two parts: the GAL4 gene, encoding the yeast transcription activation protein gal4, and the UAS (Upstream Activation Sequence), an enhancer to which GAL4 specifically binds to activate gene transcription. This GAL4 gene is placed under the control of a selected gene promoter, or driver gene, while the UAS controls the expression of a target gene, or RNAi construct. Only if these two factors are present in the same cell, UAS promoter-driver-gene or RNAi construct, is expressed. In this manner, RNAi can be targeted to appropriate cell populations and investigate whether expression of a specific gene is required for a normal toll pathway in vivo. The short hairpin (sh) RNAs was engineered to suppress the expression of specific toll after crossing to insects carrying proper tissue or cell-specific inducible drivers. We used GAL4/UAS system, a biochemical method used to study gene expression and function in organism of *Drosophila*. GAL4 encodes a protein of 881 amino acids, identified in the yeast *Saccharomyces cerevisiae* as a regulator of genes induced by galactose. GAL4 regulates the transcription of the divergently transcribed GAL10 and GAL1 genes by directly binding to four related 17 base pair sites located between these loci. These sites define an Upstream Activating Sequences (UAS) element which is cis acting regulatory sequence, essential for the transcriptional activation of these GAL4 regulated genes. The shRNA is determinate if signals derived from

definite toll are able to regulate the development, proliferation and differentiation of specific cellular subpopulations in the nervous tissue. Initially most GAL4 drivers are characterized by crossing to a responder line containing a reporter gene, such as UAS-beta galactosidasi (UAS-LacZ) or UAS-Green Fluorescent Protein (GFP). The result of this crossing is a mutant where the target gene is silenced.

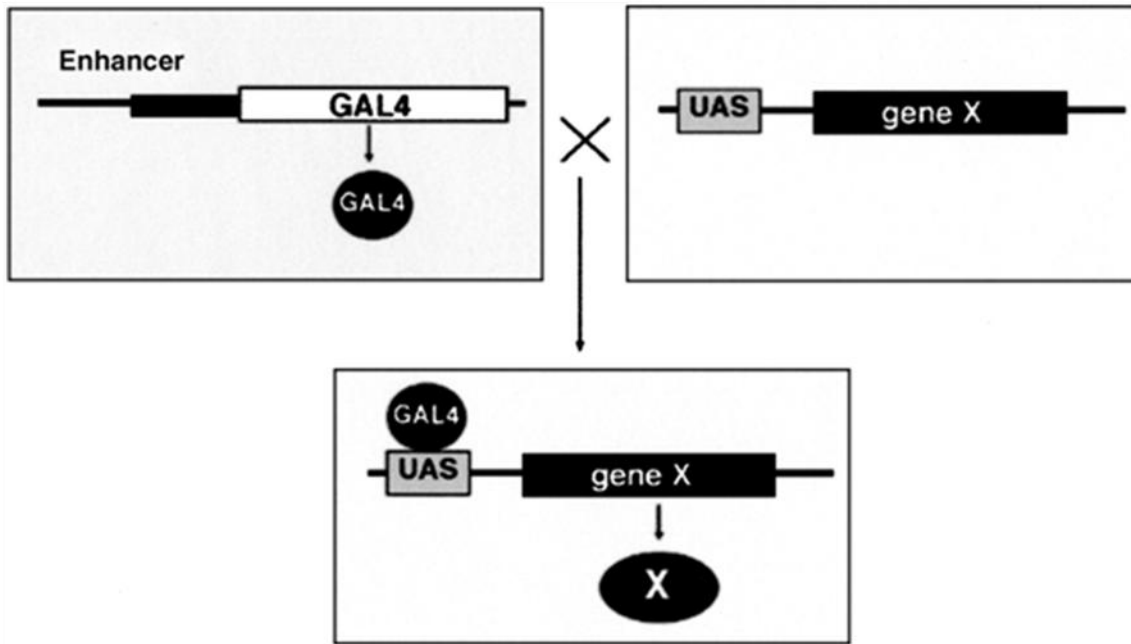


Figure 4.1 Cartoon of the UAS-GAL4 binary expression system

4.3a Temperature sensitive

We have performed two types of silencing temperature sensitive.

Initially we have worked at 29°C, ideal temperature for maximum silencing, to show that UAS-GAL4 system worked properly (**constitutive silencing**).

1. ♀ (♂) x ♂ (♀) at 29°C
2. Larval stage and pupal stage at 29°C
3. F₁ adult generation at 29°C

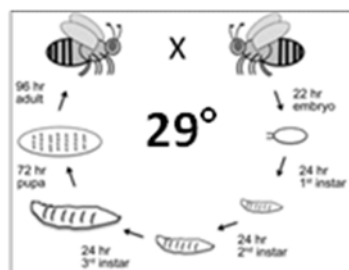


Figure 4.2 Cartoon of life cycle during constitutive silencing

4.3b Temperature inducible silencing

To exclude possible effects due to embryonic developments anomalies, after we performed temperature **inducible silencing**:

1. ♀ (o ♂) x ♂ (o ♀) at 18°C
2. Larval stage and pupal stage at 18°C
3. F₁ adult generation at 29°C for 8 days

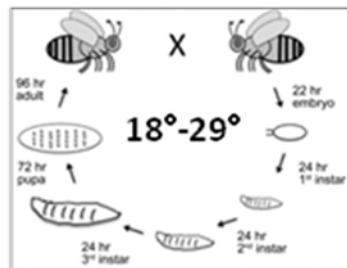


Figure 4.3 Cartoon of life cycle during inducible silencing

4.3b Chemically inducible

Afterwards we decided to use a different type of silencing: **gene switch**. The UAS-GAL4 System is the key concept but this time the silencing is controlled by a chimeric GAL4 protein that becomes active in the presence of the steroid RU486 (mifepristone) that is supplemented in the food.

1. ♀ (o ♂) x ♂ (o ♀) at room temperature (25°C)
2. Larval stage and pupal stage at room temperature
3. F₁ adult generation at room temperature
4. Administration of RU486 for 10 days at 100µg concentration

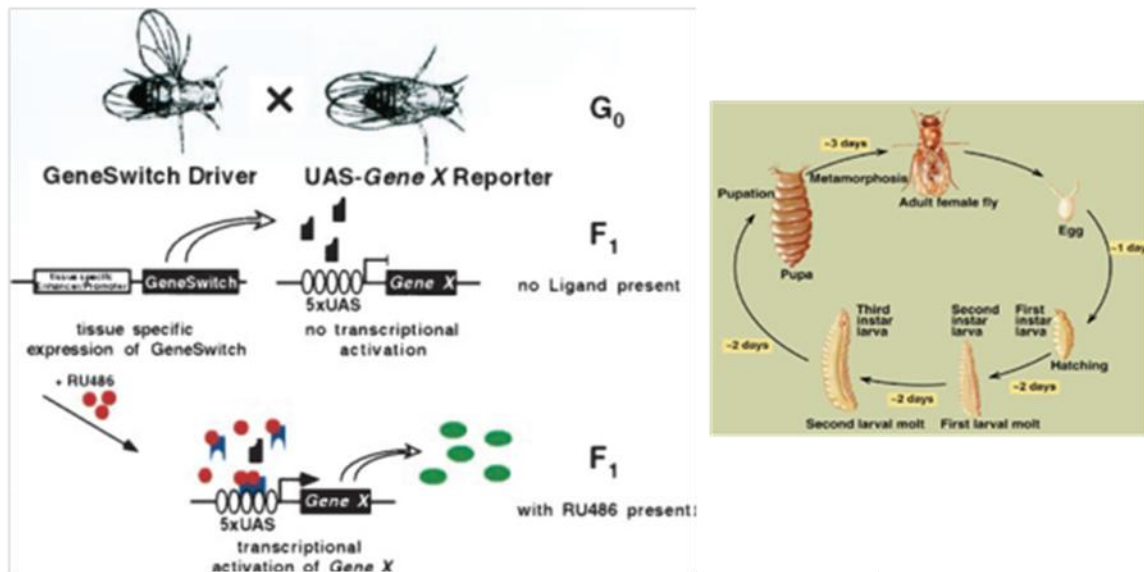


Figure 4.4 Cartoon of life cycle during chemically inducible silencing

The difference between the constitutive and inducible systems, besides the type of induction, is the time of silencing activation: in the inducible system the silencing is active only in the adult generation already formed.

4.4 Life cycle and reproduction

The life cycle of *Drosophila* consists of a series of successive steps:

- Embryonic stage
- Larva stage primary
- Larva stage secondary
- Larva stage tertiary
- Pupal stage
- Adult individual

The reproductive cycle that starts up from the embryonic stage to the adult covers a time period of about 10-12 days at a temperature of 25 °C; the adult individual is living about 50-60 days at 22-25°C.

4.5 Nutrient medium for *Drosophila melanogaster*

Individuals of *Drosophila melanogaster* were reared in a dedicated laboratory, in plastic disposable containers with foam or cotton cap, using a nutrient medium comprising:

- agar 1.2% (w / v) (BD Diagnostics)
- granulated sugar 4.4% (w / v)
- yeast extract 4.4% (w / v) (MP BioMedical)
- corn flour 4% (w / v)

in drinking water.

The nutrient medium is autoclaved and allowed to cool at 37°C, temperature at which it add the antifungal Nipagin (methyl 4-hydroxybenzoate, Sigma-Aldrich), 0.1% (w/v) dissolved in 70% ethanol (v/v), is added to the nutrient medium. The nutrient medium is then aliquoted in appropriate containers before the agar congeals.

4.6 Bowel dissection

Insects are sacrificed with CO₂. Through stereomicroscope (Nikon SMZ645) the head was cut with a special surgical scissors, placing the body on a glass slide drizzled with PBS1X to prevent drying out of the flies. . Next, we removed the gut with micro-tweezers from the back, being careful not to tear up it since it was extremely fragile. For RNA extraction each sample consisted of 30 individual guts.

4.7 RNA extraction

For extraction of total RNA from tissue it is used the OMEGA's E.Z.N.A. total RNA kit. This kit uses high-affinity mini-columns with silica gel that enable RNA purification of dimension higher of 200pb.

Briefly, TRK Lysis Buffer supplemented with β -mercaptoethanol was added to the samples and tissues were homogenized with a rotor-stator Mixer Mill MM300 (Quiagen) for 8 minutes at 20Hz. Tissues were then centrifuged at 13.000 rpm for 5 minutes to remove tissue debris. The cleared supernatant was transferred to a clean 1.5 ml centrifuge tube and an equal volume of 70% ethanol was added to the lysate and thoroughly mixed.

The samples were applied to a HiBind RNA spin column placed into a 2 ml collection tube and then centrifuged at $10,000 \times g$ for 60 seconds at room temperature. The flow-through was discarded and the column washed twice with 500 μ l of RNA Wash Buffer. RNA was eluted with 40 μ l of DEPC-treated water.

Total RNA extract was then stored at -80°C .

The amount of RNA was determined by spectrophotometric reading (Nanodrop ND-1000) at a wavelength of 260 nm, while the purity was estimated using the relationships of absorbance A_{260}/A_{280} e A_{260}/A_{230}

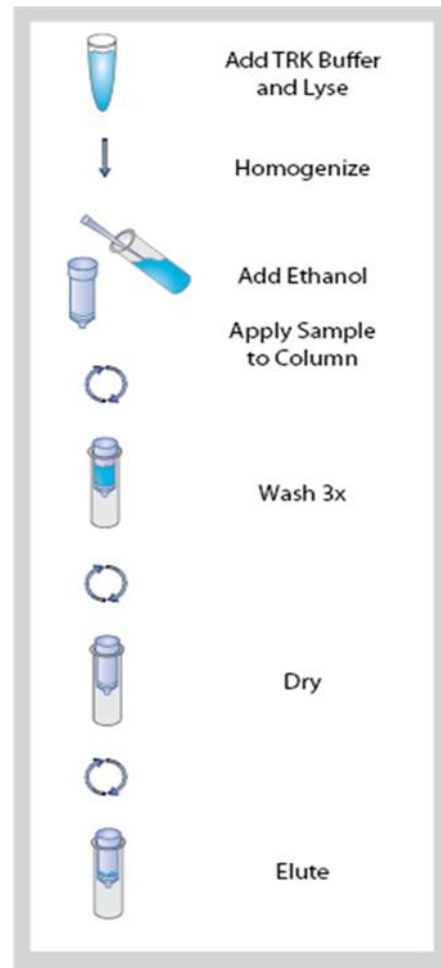


Figure 4.5 Representation of protocol

4.8 RT-PCR

The RNA purified from the flies were retrotranscribed to cDNA using the reverse transcriptase (RT) of Murine leukemia virus of Moloney, which acts in the presence of magnesium ions, and universal primers (random). For this reaction is preparing a mixture consisting in 1,5 μ l reaction buffer 10x (Tris-HCl 10mM pH 8.3, KCl 50mM), 3,3 μ l MgCl₂ 25mM, 3 μ l dNTPs 500 μ M for dNTP, 0,75 μ l random hexamers 10 μ M, 0,2 μ l RNasi inhibitor, 0,25 μ l MULV, MilliQ water to a final volume of 15 μ l including μ l of sample equivalent 500ng of RNA.

All reagents used were from Applied Biosystems.

The reverse transcription reaction was conducted in the Mastercycler thermocycler (Eppendorf) for 10 minutes at 25°C , followed by 50 minutes at 42°C and 5 minutes at 95°C . The cDNAs obtained were stored at -20°C .

4.9 RealTime-PCR

To quantify the expression of genes of interest we performed Real Time PCR assays. The experiments were conducted using the dye "SYBR Green" (Applied Biosystems®) as fluorophore. This molecule is an intercalator, that slides in between planes of base pairs in DNA. In contact with the DNA, SYBR Green undergoes a conformational change which increases the fluorescence. The amplification was conducted using the instrument ABIPRISM 7700 Sequence Detector (Applied Biosystems), equipped with a fluorimeter that recorded the fluorescence of the samples at varying number of cycles. In a typical reaction, the PCR product doubled with each cycle of amplification. Since many cycles are needed for the amplifier is detectable, the diagram fluorescence on the number of cycles exhibits a sigmoid curve. In the final cycles, the substrates reaction become scarce, the PCR products do not double and the curve begins to flatten. The point on the curve at which the amount of fluorescence assumes a value statistically significant compared to the background noise is called a cycle threshold (Ct value). The diagram of Ct of template DNA is linear, so that a comparison between the values of Ct between multiple reactions allows to calculate the concentrations of the acid nucleic acid of interest. Melting curves, following the completion of the procedure, provide an indication of the purity of the reaction product and reveal the presence of dimers of oligonucleotides or amplified nonspecific.

For this reaction is preparing a mixture consisting in 10µl SYBR® Green Master Mix 2x (Applied Biosystems), 0,25µl primer forward (fw), 0,25µl primer reverse (rv), 4 µl cDNA and DNase -free water to a final volume of 20µl.

This reaction was conducted for 2 minutes at 50°C (activation), followed by 10 minutes at 95°C (denaturation), 1 minute at 61°C (annealing) and finally 45 seconds at 72°C (extension). The last step was repeated for 42 cycles.

The quantitative differences of the various samples were normalized by means of the comparative analysis of the transgene of interest (target gene) and a housekeeping gene whose expression is constant in tissues. In experiments in *Drosophila* as housekeeping is generally used the ribosomal gene RP49.

In table 3.6 the primer pairs used for the experiments: the first one is Housekeeping gene, the second is specific neuron gene and the others toll specific.

Primer	Nucleotides sequence	T _m (°C)
RP49	ATCGGTTACGGATCGAACAA	66
	GACAATCTCCTTGCGCTTCT	68
Elav	ATGTTCTAAACGGCCTGCGA	68
	CAGCCCCGACACATAAAGGT	70
toll1	CTACGAGGATCTGGCGTTCC	72
	CCAGAGGATCGTACAGTCGC	72
toll2	AACTAACCGCCCTGGAAGG	70
	AAATGGGGCAGGGAATCAG	70
toll6	ATTTGGCACTCTGAGGAGGC	70
	GGCAAGGCCACGATTTTGTT	68
toll7	CAGCGAGCTCTACCTCTTCG	72
	GCTGTTTCAGACCACCGAGA	70
toll8	TTGTGGGTCTCAAGCGTCTC	70
	CGGCAGCTGATCGATGTAGT	70
toll9	CCATTCCCATGGTGAGCAGT	70
	AAACATGGCGGGAGTGAGAG	70

Table 4.6 Oligonucleotides *Drosophila* used. T_m= melting temperature

4.10 Immunofluorescence

Following the gut dissection, like described in 3.6 paragraph, tissues were fixed in paraformaldehyde 10% for 20 minutes. Afterwards the gut was rinsed for several time with PBS 1X to remove traces of chemical fixative. To allow a better penetration of the antibodies, the gut is placed in PBS 0.1% triton for 30 minutes. Tissues were placed in PBS-BSA 2% for 30 minutes, to block non-specific binding sites before incubation with primary antibodies: Rabbit Anti-Horseradish Peroxidase DyeLight™ 549-conjugated Affinity Pure (Jackson Immuno Research) to label neuronal bodies. At the same time tissue were incubated with Phalloidin, Fluorescein Isothiocyanate Labeled from Amanita phalloides (Sigma Aldrich) to stain actin filaments of the muscle layer of the gut. Working dilutions for different antibodies were determined by preliminary experiments. Final dilutions were as follows: anti-HRP 1:1000, phalloidin 1:2000. Antibodies were incubated for 90 minutes at 4 °C. Tissues were then washed 3-4 times in PBS to remove any residual antibody. Then the gut was mounted on slide using a fixative polymer, Moviol® 4088 (Sigma-Aldrich). The slides were then visualized by confocal microscopy (Leica TCS SP2) using the objective x40 or x63 for details.

4.11 Survival analysis

It was made survival experiment to observe the behavior of our mutants compared to a line control under physiologic conditions. From crosses kept at 18°C, selected adults of the first generation were collected every two days. Males and females were placed in separate tubes containing approximately 1 ml of jelly. Then tubes were placed at 29°C and every 48 hours the presence of dead individual was recorded. The experiment was deemed concluded when all individuals are dead. The data obtained from different experiments were summed and plotted for the two sexes separately and expressed as % survival flies for each time point.

4.12 Stress experiment with DSS

To observe the behavior of our mutants under stress conditions we feed flies a gut toxic: Dextran Sulfate Sodic (AppliChem). From crosses kept at 18°C, selected adults of the first generation, were taken and moved at 29°C for 8 days to induce maximum silencing, after that placed into tubes containing a disk of paper soaked in a solution 5% sucrose for the controls of

each line or a solution 5% sucrose + 5% DSS. Anyway tubes are placed at 29 °C and every day diskettes were changed and the number of surviving elements recorded. After 8 days of treatment, the experiment is deemed concluded. The number of data obtained are summed and plotted for a total time / live%.

4.13 Analysis of global gene expression profile following toll silencing

The samples used for this study were mutants obtained from the crossing between the line UAS-toll2 under the control of the driver ubiquitous actin-GAL4, and cellular specific elav-GAL4 (neurons), repo-GAL4 (glial cells) and mef-GAL4 (smooth muscle cells), everyone temperature inducible and w¹¹¹⁸ as control. In order to detect genes involved in the mechanism of safeguarding the SNE, it was analyzed the global gene expression profiling using microarray technology. This technology is based on the binding between two nucleic acid sequences in single-stranded complementary. A microarray consists of a solid support, typically of glass, on which are deposited probes (in *Drosophila's* case are 43,803 comprising the genes repeated more than once) that are single-stranded DNA molecules, into specific positions (spots). Each microarray has tens of thousands of spots, each of which represents a probe complementary to a single gene. The nucleic acids to hybridize to the probes anchored to the solid support, are normally obtained by marking the RNA with fluorescent molecules. Probes and targets are put in contact at a precise temperature for the hybridization to occur, and then the array is read into a scanner specific for the measurement of the fluorescent signals. The intensity of the pixels of each image is proportional to the number of probes that have hybridized probes anchored to the support. In practice, the different levels of fluorescence indicate the different levels of hybridization and then gene expression. The detected signal from the scanner is subjected to filtering algorithms and cleaning of the signal and converted into numerical values.

4.14 Evaluation of the quality and integrity of the RNA extracted from the sample

The quality and integrity of RNA extracted from the samples was assessed using the instrument Bioanalyzer 2100 (Agilent Technologies) and Agilent RNA 6000 Nano kit.

After preparing RNA Ladder (a set of six transcripts, 0.2, 0.5, 1.0, 2.0, 4.0 and 6.0 kb in length) and gel dye mix (a gel matrix added to dye concentrate) and decontaminating the electrodes (using

electrode cleaner), it load the gel dye mix in a chip using uniform pressure, distributed with a syringe, with marker and 1 μ l of sample per well and 1 μ l of ladder.

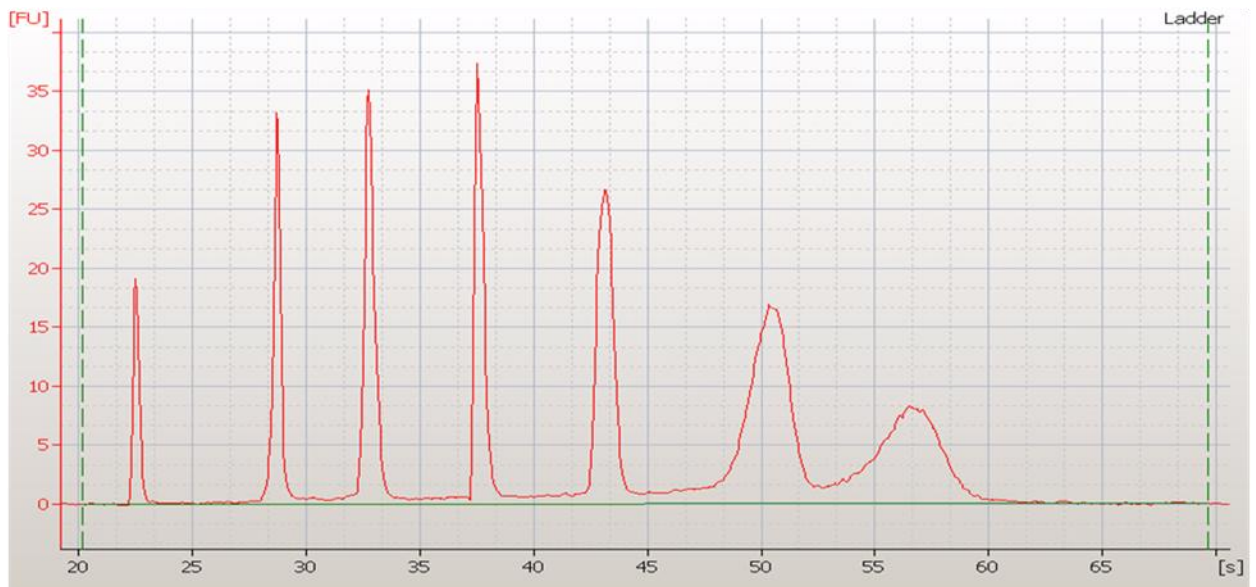


Figure 4.7 RNA 6000 nano ladder

The chip is placed for a minute in the vortex at 2400rpm (Vortexer IKA@WORKS) and then in the Agilent 2100 Bioanalyzer to fulfill the trouble. The bioanalyzer has 2100 Expert software for the extrapolation of results.

This technology, based the use of special chips, is particularly useful for the rapid analysis of nucleic acids. The chip is the support in which the samples are dispensed and is made from glass microchannels connected to each other, containing the power supplies voltage that allow the instrument to achieve more separations finely controlled. Depending on their molecular weight RNA is separated inside the microchannels and identified through the determination of the laser-induced fluorescence, detected between 670-700 nm. The use of the dye capable of intercalation between the nucleobases in combination with the determination of fluorescence used by the system is able to detect concentration difference between the various samples, also very small. The software will automatically compare the samples analyzed with the ladder, to determine the concentration and identify ribosomal peaks present. The results are presented both as separate bands on gels, and as a graph on Cartesian axes.

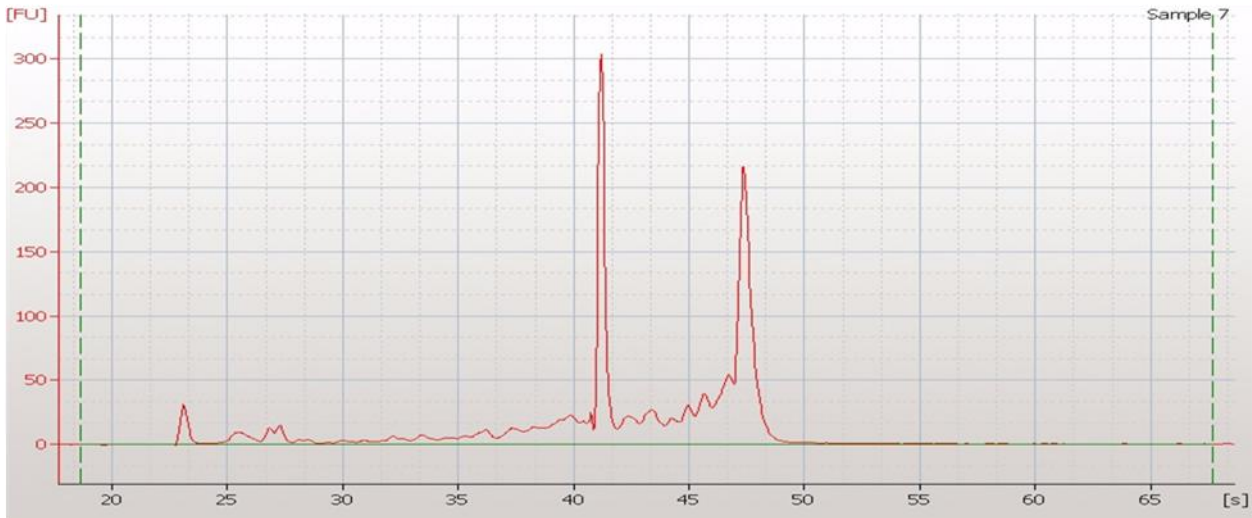


Figure 4.8 RNA peaks sample run

The first shows two clearly separated bands corresponding to ribosomal units 18S and 28S as a function of separation time in seconds. Between the data provided by the instrument, relevant is the RIN (RNA Integrity Number) that is generated for each sample and indicates the quality of RNA analyzed: can have a value between 1 (completely degraded RNA) and 10 (RNA perfectly intact and of good quality). The optimal value of RIN is between 7 and 8, in this condition, the RNA can be used for subsequent experiments. In the study all the chips have been prepared according to the protocol provided dall'Agilent described before.

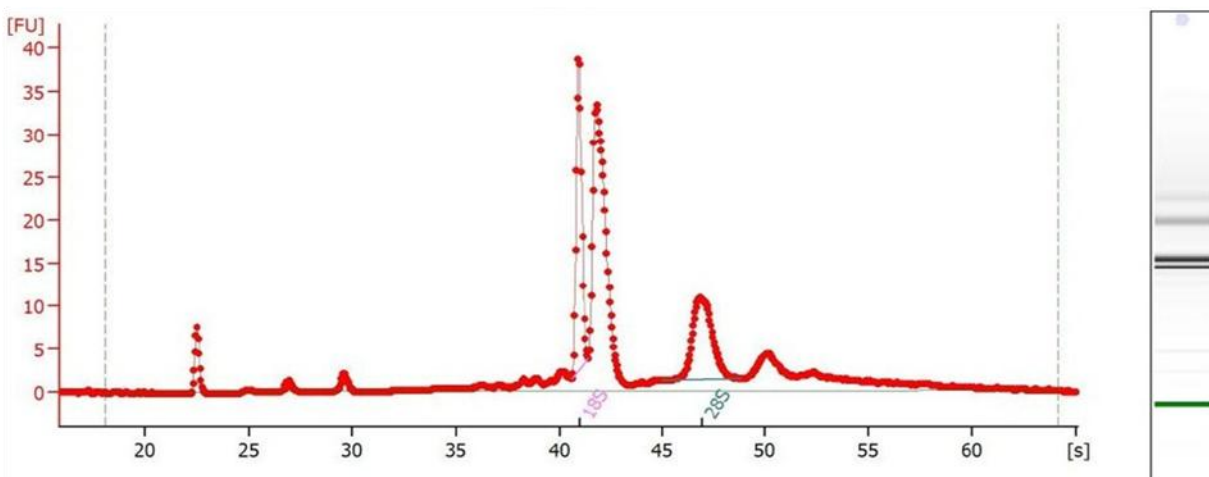


Figure 4.9 Representative image of graph on Cartesian axes, result of Agilent 2100 Bioanalyzer. Two clearly separated bands corresponding to ribosomal units 18S (two peaks for drosophila specie) and 28S as a function of separation time in seconds, using for calculate RIN (RNA Integrity Number).

4.15 Analysis of global gene expression profiling using microarrays

The labeling reaction of RNA obtained from the samples was performed according to the protocol Quick Amp labeling kit (Agilent Biotechnologies). This kit allows to generate a cRNA labeled with the fluorescent dye Cy3. The method is based on the use of T 7 RNA polymerase that simultaneously amplifies target material and incorporates cyanine 3-CTP.

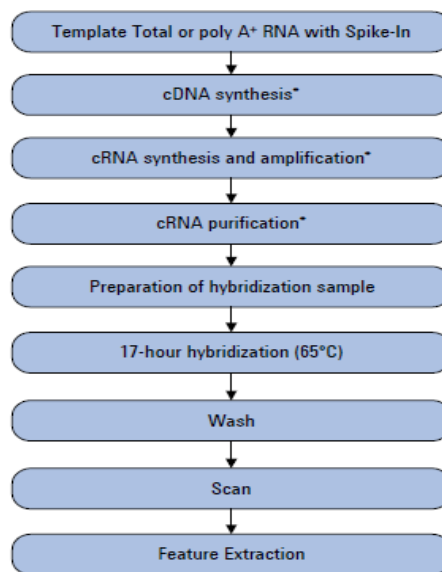


Figure 4.10 Workflow for sample preparation and array processing

-SAMPLE PREPARATION:

The set of input total RNA was 200 ng/1,5 µl. To each sample were added 1.2 µl of T7 promoter primer, and 2 µl of the dilution of spike mix and DEPC water until 11.5µl total volume and were made to incubate at 65 ° C for 10 minutes. The Spike-Mix is a solution containing ten *in vitro* synthesized polyadenylated transcripts, at concentrations from 1 to 6 in logarithmic scale which is an internal control for normalization.

-SUMMARY OF DOUBLE-STRAND cDNA:

The sample thus prepared is then converted to double stranded cDNA using a reverse transcriptase (MMLV RT).

The cDNA synthesis included a mixture cDNA Master Mix consisting in 4µl of 5X First Strand Buffer, 2µl of 0,1M DTT, 1µl of 10mM dNTP mix, following the addition of two enzyme: 1µl of MMLV-RT and 0,5µl of RNase-OUT for a total volume of 8,5µl for each reaction.

The reaction was conducted in the Mastercycler thermocycler (Eppendorf) for 2 h at 40°C, then 15 min at 65°C and cooling on ice for 5 min.

- SUMMARY OF SHARP cDNA:

In this phase the product is labeled cDNA. The mixture Transcription Master Mix for synthesis of cRNA consisting in 15,3µl of Nucleasi free water, 20µl of 4X transcription buffer, 6µl of 0,1 M DTT, 8µl of NTP mix, 6,4µl of 50% PEG, following the addition of three enzyme 0,5µl of RNase OUT, 0,6µl of Inorganic Pyrophosphatase and 0,8µl of T7 RNA polymerase.

The marking is done by Cyanina3 (Cy3), in the amount of 2,4µl.

The reaction was conducted in the Mastercycler thermocycler (Eppendorf) for 2 h at 40°C.

-PURIFICATION AND QUANTIFICATION OF SHARP cDNA:

Purification of labeled cDNA was carried out following the protocol of the kit "RNeasy Minikit" (Quiagen).

Briefly, it add nuclease-free water, Buffer RLT and ethanol 96% to sample and mix well pipetting.

It transfer the cRNA sample to an Rneasy Mini Spin Column and spin in a centrifuge at 4°C for 30seconds at 13000 x g

It add Buffer RPE (containing ethanol) to the column and spin in a centrifuge at 4°C for 60seconds at 13000 x g for two times

It elute the purified cRNA sample add Rnase-Free Water directly onto the membrane.

Wait 60seconds, then centrifuge at 4°C for 30seconds at 13000 rpm.

Quantification of labeled cRNA and the incorporation of the cyanine were carried out by spectrophotometer reading Nanodrop1000 (Thermo Scientific). The instrument in addition to the concentration for cRNA labeled and the amount of Cy3 present, is able to provide the absorbance ratios 260/280 (measure of protein contamination) and 260/230 (measure contamination of solvents). On the basis of the values of concentration of labeled.

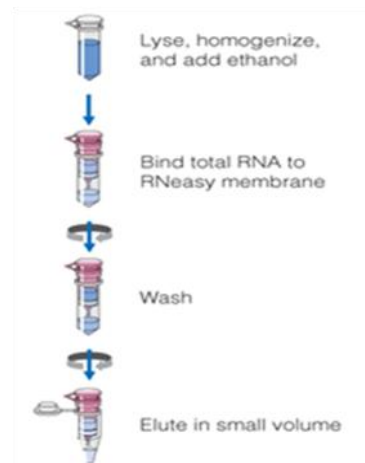


Figure4.11Purification the labeled

-MARKED ON THE HYBRIDIZATION cRNA MICROARRAY

The step of hybridization of the samples on the slides containing the probes was conducted following the indications of Gene Expression Hybridization Kit.

This step includes preparation of a mixture Fragmentation mix with 1,65µl of Cy3-labeled, 11 µl of 10X Blocking Agent, 2,2 µl of 25X fragmentation Buffer and Nuclease- free water to 55 µl.

The reaction was conducted in the Mastercycler thermocycler (Eppendorf) at 60°C for 30 minutes.

After which were added 55 µl GEx of 2X Hybridization Buffer to stop the reaction.

At this point the hybridization of the sample can initiate, which involves the use of a slide containing the probes (Agilent microarrays , or active slide) and a slide support (inactive slide, slide or gasket). Are then deposited 100 µl on the sample to hybridize gasket slide taking care not to deposit bubbles and then is placed over this the active part (microarrays); the bedroom hybridization is thus obtained is closed and placed in a rotating oven at 65 °C for 17h.

At the end of the period of hybridization the microarray is separated gasket from the slide and are carried out two washes of one minute each with two different washing buffer (respectively GE buffer1 wash at RT and GE wash buffer 2 at 37°C) . The slide is then placed in a special room and proceed with the scan.

-SCANNING AND DATA EXTRACTION BY FEATURE EXTRACTION 9.1

Each slide was scanned with the Agilent Microarray Scanner and has performed data extraction by using the Feature Extraction software 9.5.1 that is able to convert scanned images and quantitative data generated by the scanner in as intensity signal.

4.16 Analysis of data obtained from microarray

The analysis of the obtained data was divided into two phases:

-Data Processing, was to evaluate the quality of data, in the background subtraction, and research in the normalization of outlier values.

-Data Analysis, which included identifying differential gene expression, analysis of clustering. The first part was made possible thanks to the Feature Extraction 9.1 software, which automatically makes the gridding (identification of each spot), segmentation (dividing the pixels belonging to the fore and background) and the extraction of signal intensity (median of pixels) to extract the raw data signal intensity and background and to provide a report on the quality of the microarray.

From the analysis of these summaries, QC report, were evaluated a number of characteristics that are used for the determination whether the microarray can be considered of good quality or not, and then we can proceed with the analysis. In particular, evaluating the distribution of the outlier, the presence of gradients of intensity of the signal, the state of the negative controls, the quality of the replicas intra-array.

It has been subsequently determined the relative intensity of each spot of the array with respect to the median of the values of the same spot on all arrays analyzed. As the results of the processing we have observed that all arrays were of good quality.

Once collected the raw data from Feature Extraction 9.1, we used the program GeneSpring 13.0, software with content and visualizations for research and drug discovery in genomics, metabolomics, and proteomics.

4.17 Statistical Analysis

Data are reported as mean \pm standard error of the mean . The statistical significance was calculated using the Student t test, analysis of variance one -way ANOVA and Bonferroni test, using the software GraphPad Prism 4.00. For survivor analysis we used the software MedCalc 9.2, the meaningfulness was calculated using Wilcoxon-Mann-Whitney test: comparison of the averages of two independent groups of samples, of which we can't assume a distribution of Gaussian type.

Were considered statistically significant results with values of $p < 0.01$.

For microarray analysis instead we used GeneSpring 13.0, in particular for statistical analysis Benjamini Hockberg test that based on FDR (False Discovery Rate) connected to P-value < 0.05 and Bonferroni method is a simple method that allows many comparison confidence intervals $p < 0.05$ while still assuring an overall confidence coefficient is maintained

5 RESULTS

5.1 Efficiency of temperature sensitive GAL4 drivers

Initially we tested the efficiency of drivers GAL4, both ubiquitous (actin and tubulin) and cellular specific (neurons, glia and smooth muscle cells) by crossing the specific GAL4 lines with a UAS line expressing the green fluorescent protein. Flies were dissected and the gut observed using confocal fluorescence microscopy. GFP expression was homogeneous using the ubiquitous actin and tubulin, and among them GFP expression was stronger with the tubulin driver. Cell specific drivers induced GFP expression with a pattern that was well-suited to the different drivers: *mef* for smooth muscle allowed to visualize the muscle cell through the bowel, whereas *elav* and *repo* lighted few cells in the gut wall (figure 5.1).

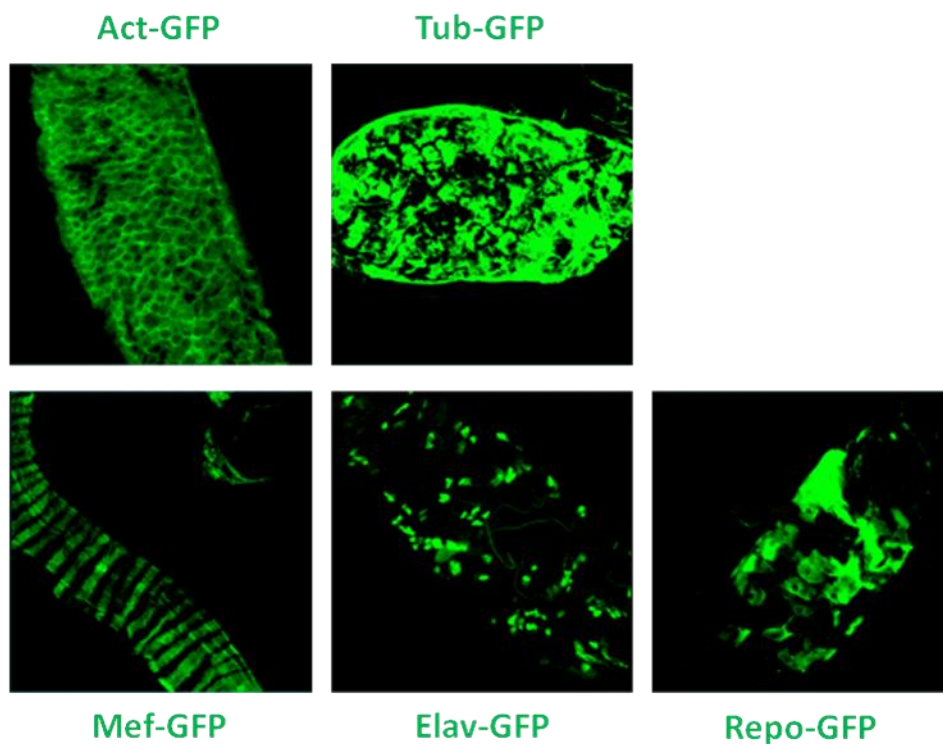


Figure 5.1 Immunofluorescent of midgut. GFP expression of GAL4 drivers in green: actin and tubulin (ubiquitous), *mef* (smooth muscle cells), *elav* (neurons), *repo* (glial cells). Tissue were visualized using confocal microscopy. Scale bar 75 μm .

5.2 Reduced expression of different *toll* using ubiquitous driver actin

To determine the level of gene silencing obtained in lines expressing toll-specific siRNA under the control of the ubiquitous driver actin, we quantified toll mRNA by real time RT-PCR. As housekeeping gene we used the RP49 gene, which codes for a ribosomal protein. From real time RT-PCR data we observed a silencing of more than 80% for the different toll, except for Toll6 (Figure 5.2) whose silencing was ineffective.

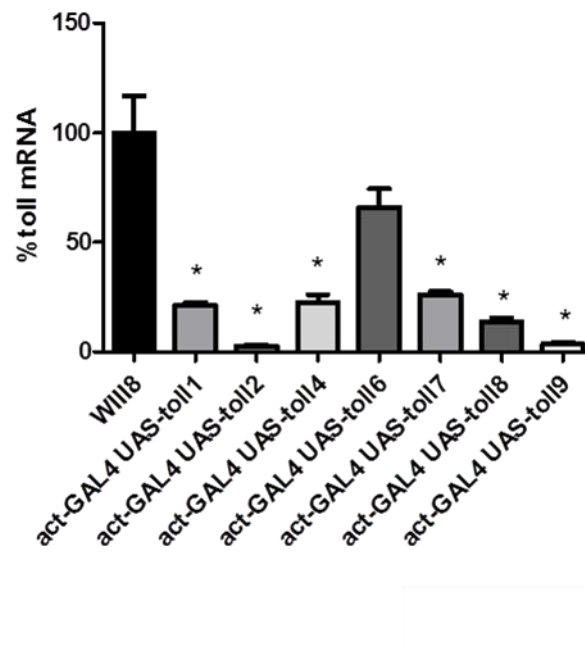


Figure 5.2 Toll mRNA level determined in the gut of *Drosophila* lines by qRT-PCR. (n= 3 experiments combining 20-30 gut flies).
* P<0.001 versus W¹¹¹⁸

4.3 Ubiquitous *toll* silencing causes loss of intestinal neurons

To determine that the loss of tolls, by constitutive silencing, has an effect on the intestinal neuronal integrity, we performed immunohistochemical analysis on the intestine of *Drosophila*. By staining with the neuronal marker Horseradish Peroxidase (HRP) we observed a depletion in intestinal neurons in mutants where we silenced tolls using the ubiquitous driver actin as compared to line control w¹¹¹⁸ (Figure 5.3, 5.4, 5.5, 5.6). Looking at the representative images it is evident a more pronounced neuronal depletion in toll2 and toll9 silenced.

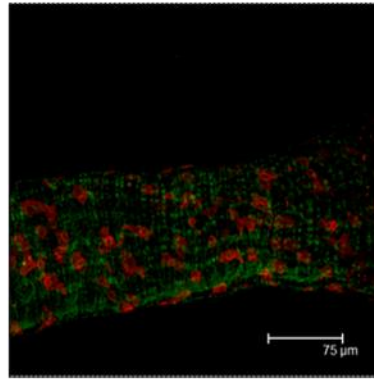


Figure 5.3 Representative images of immunofluorescence analysis performed on midgut of w^{1118} control for HRP (neurons, in red) and phalloidin (smooth muscles, in green). Scale bar: 75 μm .

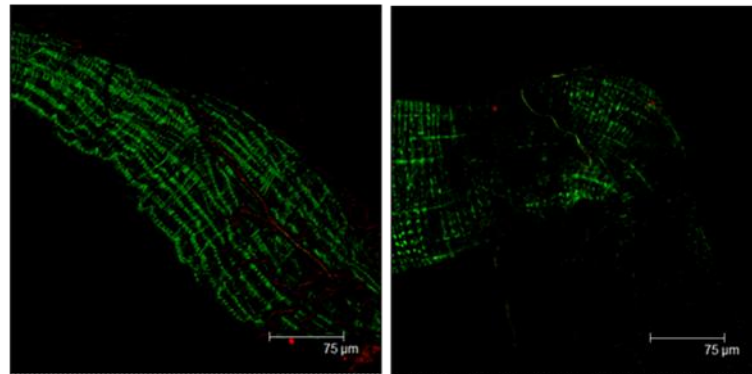


Figure 5.4 Representative images of immunofluorescence analysis performed on midgut of actGAL4 UAS-toll2 and actGAL4 UAS-toll9 for HRP (neurons, in red) and phalloidin (smooth muscles, in green). Scale bar: 75 μm .

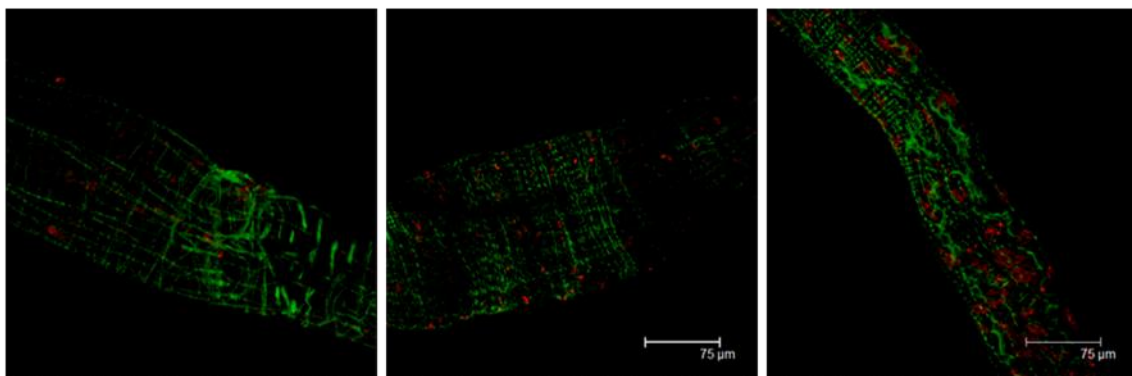


Figure 5.5 Representative images of immunofluorescence analysis performed on midgut of actGAL4 UAS-toll1, actGAL4 UAS-toll4 and actGAL4 UAS-toll6 for HRP (neurons, in red) and phalloidin (smooth muscles, in green). Scale bar: 75 μm .

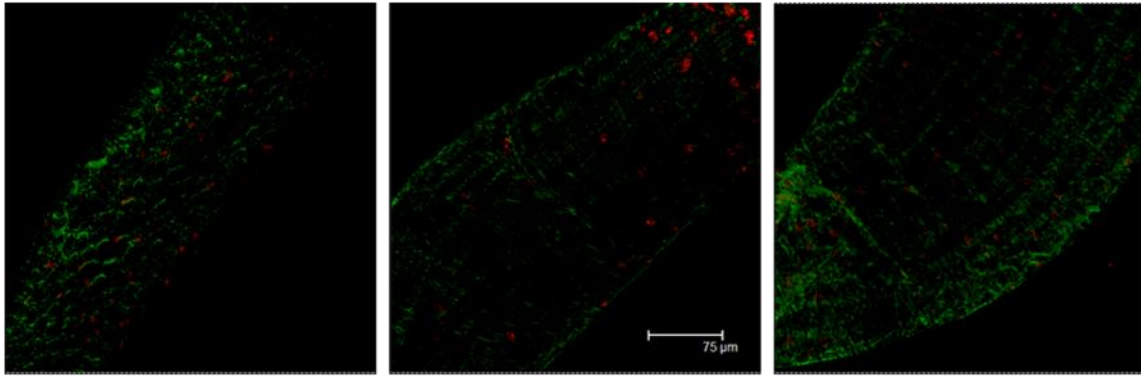


Figure 5.6 Representative images of immunofluorescence analysis performed on midgut of actGAL4 UAS-toll7, actGAL4 UAS-toll8 and actGAL4 UAS-Myd88 for HRP (neurons, in red) and phalloidin (smooth muscles, in green). Scale bar: 75 μ m.

5.4 Temperature inducible *toll* silencing

To exclude that the observed neuronal loss was the consequence of toll silencing during embryonic development, we switched to a temperature inducible system and focused on toll2 and toll9 lines, in which we have observed the most severe neuronal anomalies. Thus, first we verified the level of toll silencing and then the changes in neuronal number of flies raised at 18°C (no silencing) and then moved on at 29°C. In these experiments the effect of silencing was determined at $t = 0$ (at the time of transfer from 18 °C to 29 °C), after 4 days and after 8 days at 29°C.

As shown in Figure 5.7 by crossing UAS-toll2 and UAS-toll9 lines with the ubiquitous driver actin, different levels of silencing were obtained depending on the temperature. A minimal silencing was observed at 18°C, whereas at 29°C a silencing comparable to the constitutive one was measured.

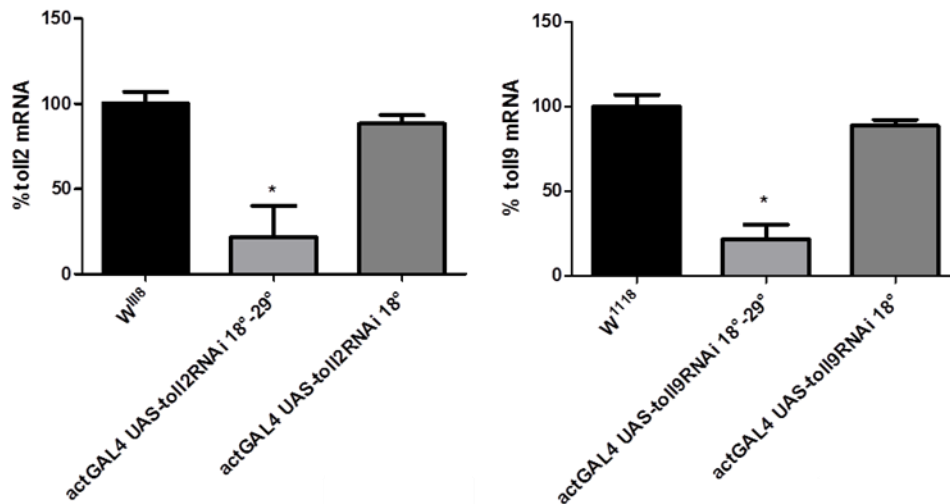


Figure 5.7 toll2 and toll9 mRNA level determined in the gut of *Drosophila* mutants by qRT-PCR (n= 3 experiments combining 20-30 gut flies). * P<0.001 versus W¹¹¹⁸

As shown in the representative immunofluorescence respect control in figures 5.8, the HRP⁺ immunostaining of midgut neurons was drastically reduced in actGAL4 UAS-toll2 and actGAL4 UAS-toll9 after 4 days and almost completely disappeared after 8 days in figure 5.9 and 5.10.

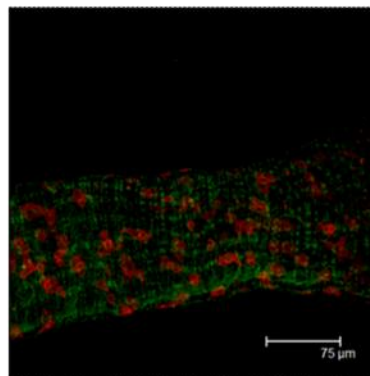


Figure 5.8 Representative images of immunofluorescence analysis performed on midgut of W¹¹¹⁸ control for HRP (neurons, in red) and phalloidin (smooth muscles, in green). Scale bar: 75 μm.

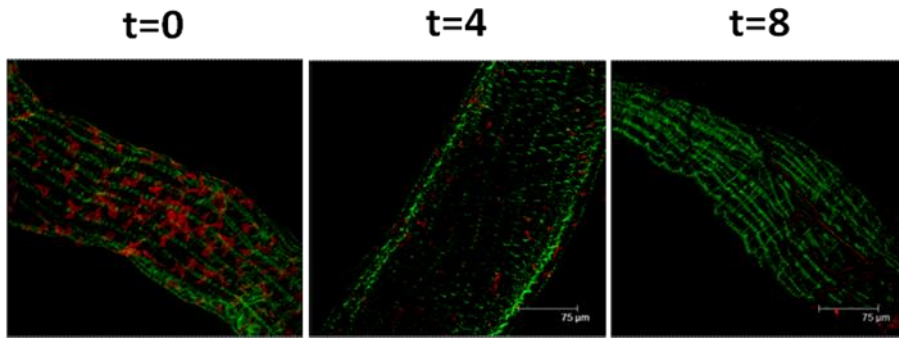


Figure 5.9 Representative images of immunofluorescence analysis performed on midgut of actGAL4 UAS-toll2 for HRP (neurons, in red) and phalloidin (smooth muscles, in green) at time t=0 (no silencing), t=4 (four days after moving from 18°C to 29°C) and t=8 (eight days after moving from 18°C to 29°C). Scale bar: 75 μm.

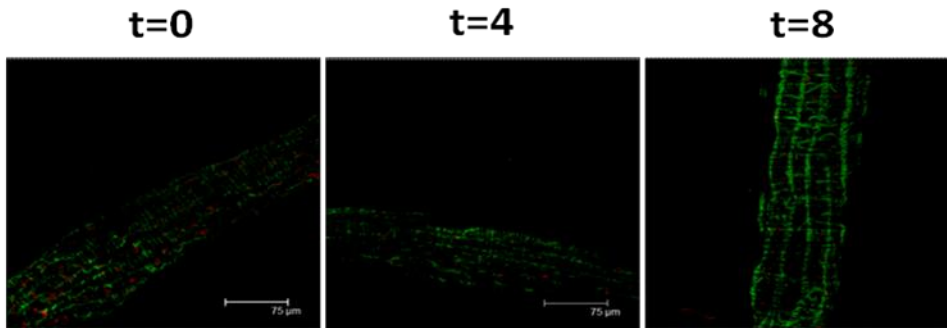


Figure 5.10 Representative images of immunofluorescence analysis performed on midgut of actGAL4 UAS-toll9 for HRP (neurons, in red) and phalloidin (smooth muscles, in green) at time t=0 (no silencing), t=4 (four days after moving from 18°C to 29°C) and t=8 (eight days after moving from 18°C to 29°C). Scale bar: 75 μm.

The direct quantification of HRP^+ neurons in the flies midgut with toll2 and toll9 silencing using the ubiquitous driver actin showed a significant reduction of neuronal bodies after 4 days at 29°C, that was more pronounced at 8 days (Figures 5.11).

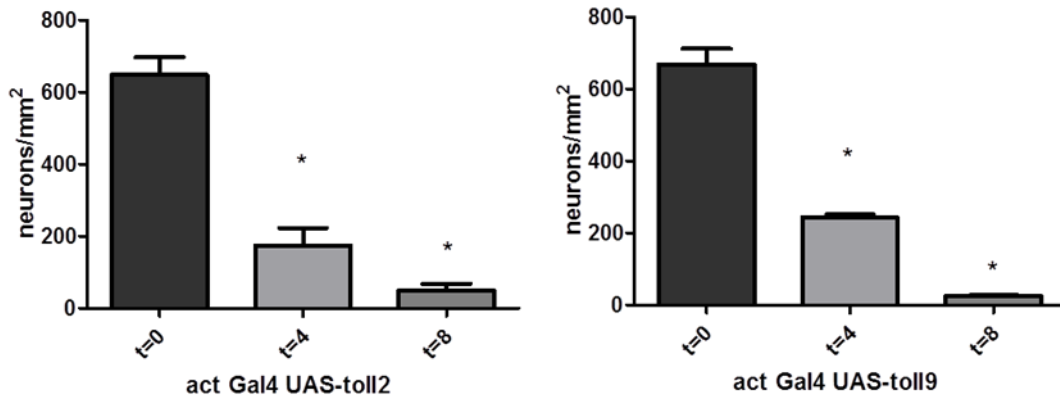


Figure 5.11 Quantification of neurons in the midgut of act GAL4 UAS-toll2 at time t=0 (no silencing), t=4 (four days after moving from 18°C to 29°C) and t=8 (eight days after moving from 18°C to 29°C) expressed as neurons/mm². * p<0.01 versus W¹¹¹⁸

To exclude driver-specific effects we performed similar studies using a second ubiquitous driver, tubulin. As shown in Figures 5.13 and 5.14 also using the tubulin driver to direct toll2 and toll9 silencing we obtained a drastic reduction in neuronal cell bodies after 4 and 8 days.

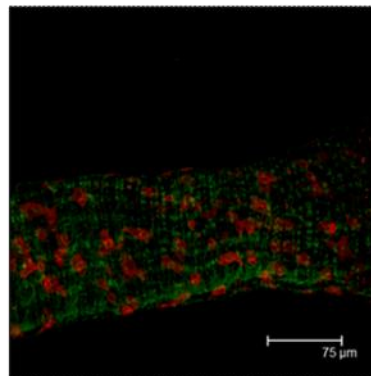


Figure 5.12 Representative images of immunofluorescence analysis performed on midgut of W¹¹¹⁸ control for HRP (neurons, in red) and phalloidin (smooth muscles, in green). Scale bar: 75 μm.

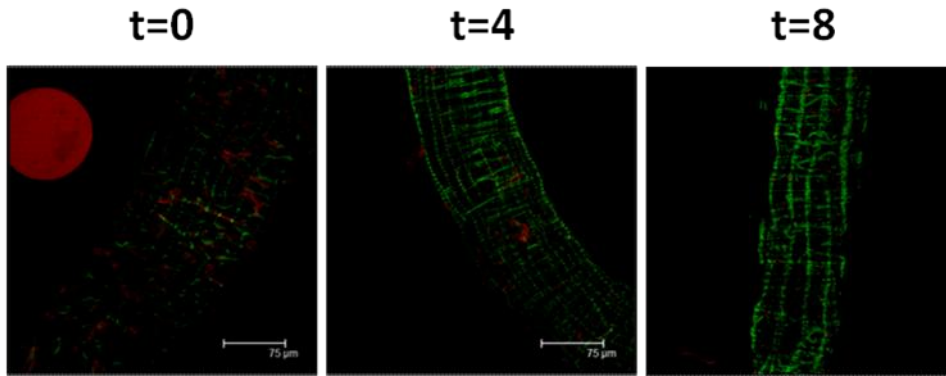


Figure 5.13 Representative images of immunofluorescence analysis performed on midgut of tubGAL4 UAS-toll2 for HRP (neurons, in red) and phalloidin (smooth muscles, in green) at time t=0 (no silencing), t=4 (four days after moving from 18°C to 29°C) and t=8 (eight days after moving from 18°C to 29°C). Scale bar: 75 μm.

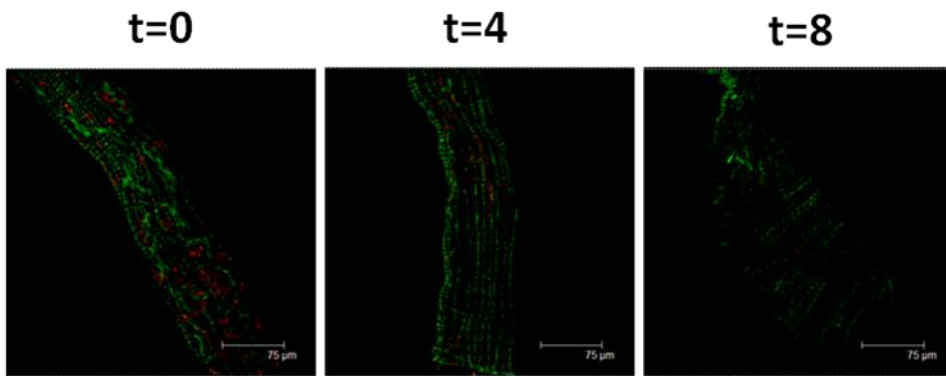


Figure 5.14 Representative images of immunofluorescence analysis performed on midgut of tubGAL4 UAS-toll9 for HRP (neurons, in red) and phalloidin (smooth muscles, in green) at time t=0 (no silencing), t=4 (four days after moving from 18°C to 29°C) and t=8 (eight days after moving from 18°C to 29°C). Scale bar: 75 μm.

The direct quantification of HRP^+ neurons in the flies midgut with toll2 and toll9 silencing using the ubiquitous driver tubulin showed a significant reduction of neuronal bodies after 4 days at 29°C, that was more pronounced at 8 days (Figures 5.15).

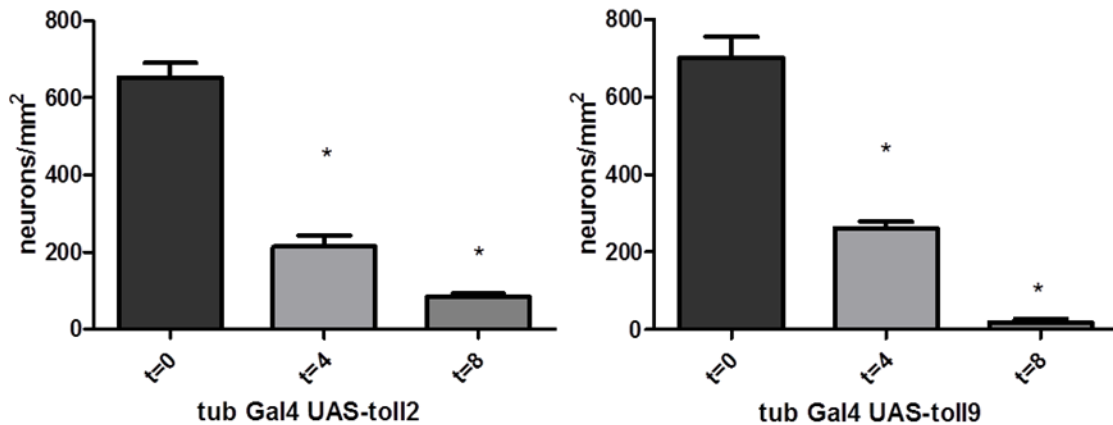


Figure 5.15 Quantification of neurons in the midgut of tub GAL4 UAS-toll2 at time t=0 (no silencing), t=4 (four days after moving from 18°C to 29°C) and t=8 (eight days after moving from 18°C to 29°C) expressed as neurons/mm². * p<0.01 versus w¹¹¹⁸

5.5 Cellular specific *toll* silencing causes loss of intestinal neurons

We decided to focus on *toll2*, to investigate the weight of different cell populations on *toll2* expression. Thus we generated *Drosophila* lines carrying *toll2* silencing in a cell-specific manner, namely neurons using the *elav* driver, smooth muscle cells using the *mef* driver and glial cells using the *repo* driver. As shown in Figure 5.16, the level of *toll2* silencing in mutant lines using cellular specific drivers is less pronounced using *repo* and *elav* drivers as compared to the *mef* driver.

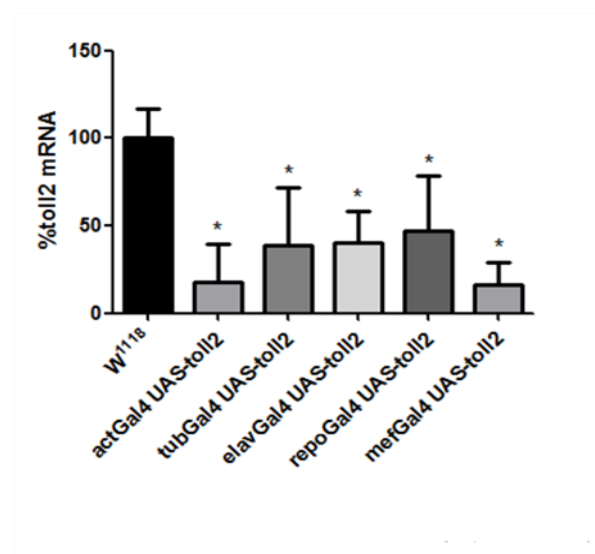


Figure 5.16 Toll2 mRNA level determined in the gut of *Drosophila* lines by qRT-PCR. (n= 3 experiments combining 20-30 gut flies). * P<0.001 versus w¹¹¹⁸

By immunofluorescent analysis of neurons in the flies midgut it is showed a significant reduction of HRP⁺ neuronal bodies respect line control (Figure 5.17, 5.18). Although toll silencing was less pronounced in the graph above respect cellular specific, the proportion of neuronal loss was the same.

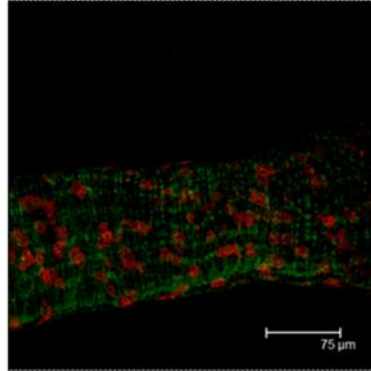


Figure 5.17 Representative images of immunofluorescence analysis performed on midgut of w^{1118} control for HRP (neurons, in red) and phalloidin (smooth muscles, in green). Scale bar: 75 μm .

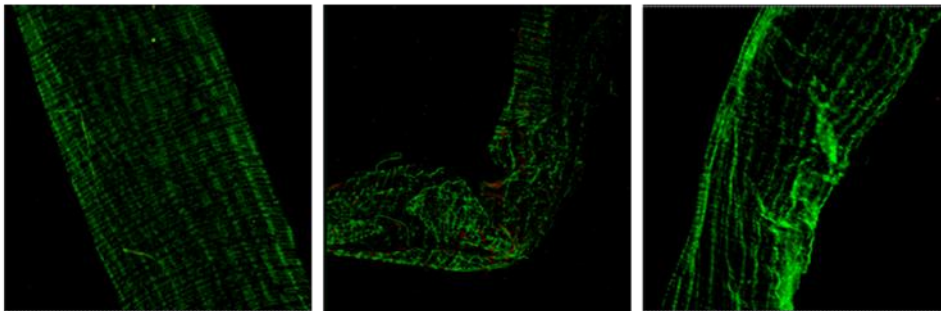


Figure 5.18 As shown in the representative immunofluorescence analysis respect line control in figures 4.17, the HRP⁺ immunostaining of midgut neurons was drastically reduced in *elav GAL4 UAS-toll2*, *mef GAL4 UAS-toll2*, *repo GAL4 UAS-toll2*.

The direct quantification of HRP⁺ neurons in the flies midgut with *toll2* silencing using the different driver either ubiquitous and cellular specific, showed a significant reduction of neuronal bodies after 8 days at 29°C (Figures 5.19).

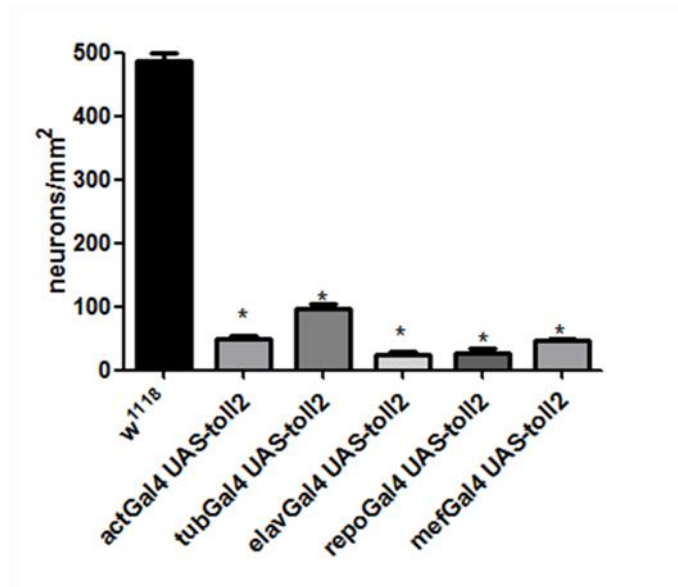


Figure 5.19 Quantification of neurons in the midgut ubiquitous and cellular specific toll2 at time t=8 (eight days after moving from 18°C to 29°C) expressed as neurons/mm². * p<0.01 versus w¹¹¹⁸

To further confirm this neuronal loss we quantify the elav mRNA by real time RT-PCR. Elav is gene spreads along nerve tissue and is more precisely located at the nuclear level. As housekeeping gene we used the RP49 gene, which codes for a ribosomal protein. From real time RT-PCR data we observed a silencing of more than 80% for the different toll.(Figure 5.20)

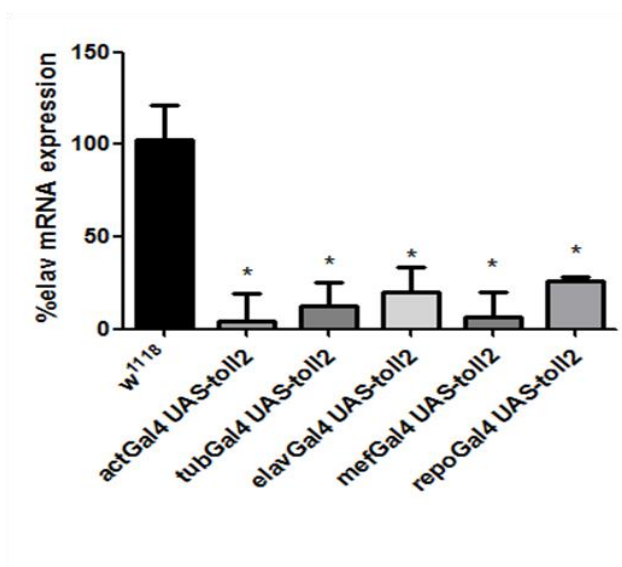


Figure 5.20 Elav mRNA level determined in the gut of Drosophila lines by qRT-PCR (n=3 experiments combining 20-30 guts flies) p<0.001 versus w¹¹¹⁸

5.6 Survival of flies carrying *toll2* silencing

The survival analysis were performed on large experimental cohorts to obtain reliable data. The control flies w^{1118} showed a shorter survival as compared to *toll2* silenced flies using both the ubiquitous actin and tubulin driver (figure 4.20 a). Similar data were obtained in flies in which *toll2* expression was silenced using cellular specific drivers: *elav* (for neurons), *mef* (for smooth muscle cells) and *repo* (for glial cells) in figure 4.20 (b e c). Thus, while in w^{1118} 50% survival was reached at 24 days, flies carrying *toll2* silencing under the ubiquitous drivers actin and tubulin showed a mean survival of 37 and 39 days respectively. Similarly, mean survival of *toll2* silenced using cell specific drivers was increased to a maximum of 43 days using the glial driver *Repo*.

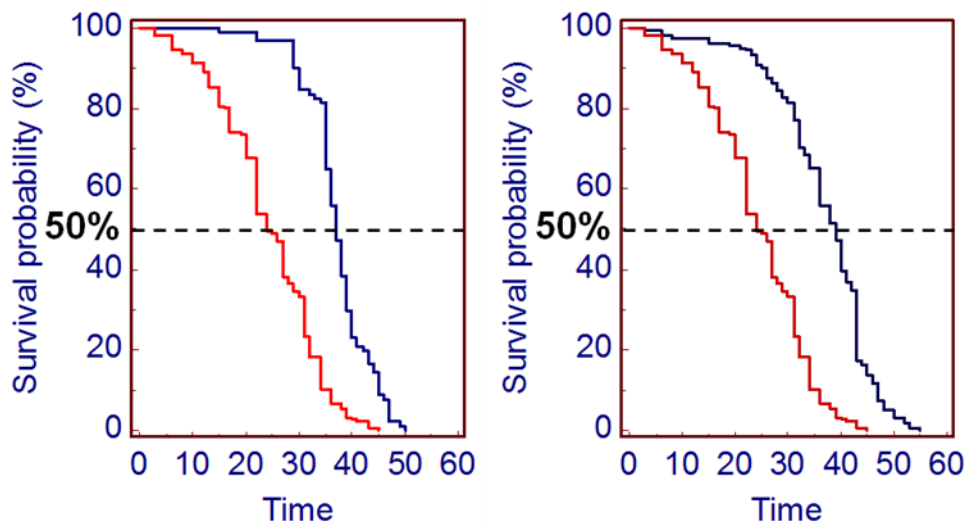


Figure 5.21a Survival curves *toll2* mutants, in red lines control w^{1118} and in blue ubiquitous silenced act *Gal4 UAS-toll2* and tub *Gal4 UAS-toll2*

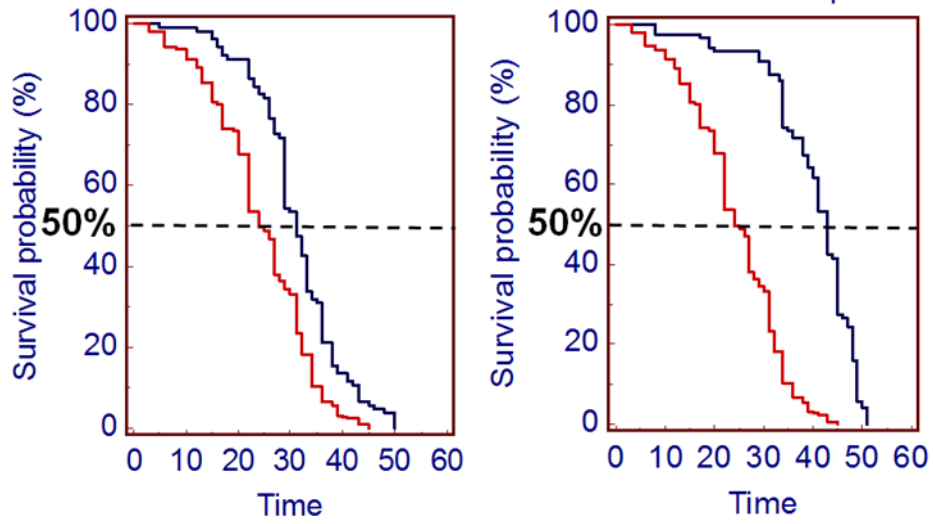


Figure 5.21b Survival curves toll2 mutants, in red lines control w^{1118} and in blue ubiquitous silenced $elavGal4$ UAS-toll2 and $repo$ Gal4 UAS-toll2

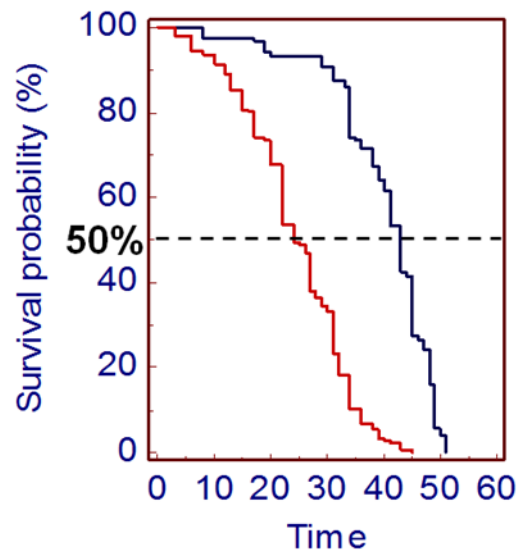


Figure 5.21c Survival curves toll2 mutants, in red lines control w^{1118} and in blue ubiquitous silenced $repo$ Gal4 UAS-toll2

In the table 5.22 are summarized the sample size and the median survival of each group.

Experimental group	Sample size	Median survival (days)
Ctrl	252	24
Act Gal4 UAS-toll2	91	37
Elav Gal4 UAS-toll2	103	31
Mef Gal4 UAS-toll2	138	41
Repo Gal4 UAS-toll2	120	43
Tub Gal4 UAS-toll2	161	39

Table 5.22 experiment data on survival curves, in the first column mutants type, in the second number of individuals, in the third median survival (days).

5.7 Survival of toll2-silenced flies following exposure to DSS

Exposure to the high molecular weight sugar DSS damage the intestinal mucosa, such as in mammals, causing the death of the flies within few days. Thus, control w^{1118} died within seven days of DSS exposure with a 50% survival rate of 5 days. Exposure of flies carrying toll2 silencing produced different phenotypes depending on the driver used. Thus, flies carrying toll2 silencing using the actin driver showed a survival rate comparable to w^{1118} whereas flies carrying toll2 silencing using the tubulin driver showed a shorter survival rate (Figure 5.23a). Indeed the latter showed a 50% survival rate of 4 days, significantly different than w^{1118} . Interestingly, using the three cellular specific drivers the survival rate in these mutant flies was higher than controls (Figure 5.23b).

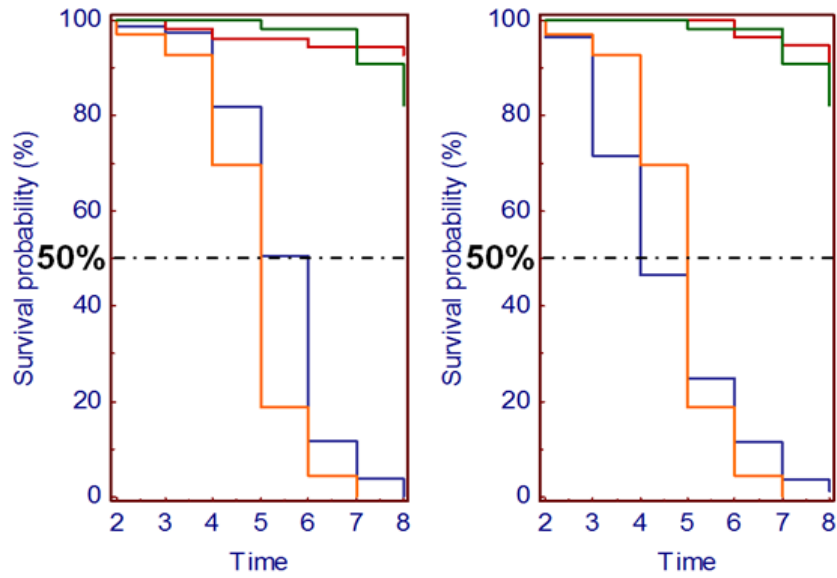


Figure 5.23: Survival curves toll2 mutants, in yellow lines control w^{1118} with DSS 5% and in green w^{1118} with sucrose 5%, in blue ubiquitous silenced act Gal4 UAS-toll2 and tub Gal4 UAS-toll2 with DSS 5%, in red act Gal4 UAS-toll2 and tub Gal4 UAS-toll2 with sucrose 5%.

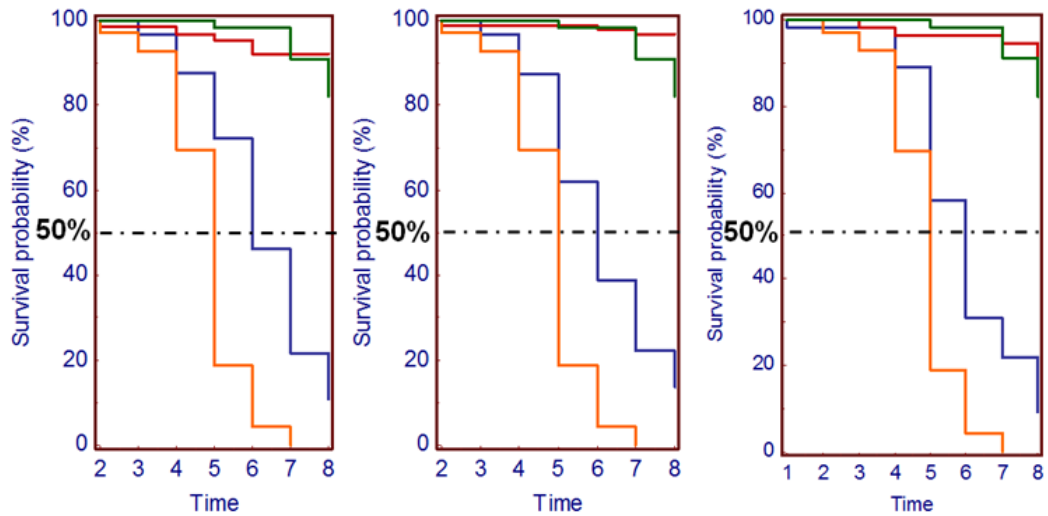


Figure 5.23b: Survival curves toll2 mutants, in yellow lines control w^{1118} with DSS 5% and in green w^{1118} with sucrose 5%, in blue cellular specific silenced elav Gal4 UAS-toll2, mef Gal4 UAS-toll2 and repo Gal4 UAS-toll2 with DSS 5%, in red elav Gal4 UAS-toll2, mef Gal4 UAS-toll2 and repo Gal4 UAS-toll2 with sucrose 5%.

In the table 5.24 are summarized the sample size and the median survival of each group.

Experimental Group	Sample size	Median survival (days)
Ctrl	69	5
Act Gal4 UAS-toll2	56	5
Elav Gal4 UAS-toll2	65	6
Mef Gal4 UAS-toll2	95	6
Repo Gal4 UAS-toll2	55	6
Tub Gal4 UAS-toll2	88	4

Table 5.24 experiment data on survival curves, in the first column mutants type, in the second number of individuals, in the third median survival (days)

5.8 Analysis of microarray assay

Since loss of toll2 signaling following either ubiquitous or cell specific silencing caused a significant loss of neurons, we decided to identify the downstream genes modulated by toll2 signaling involved in neuronal development and/or survival. Therefore we performed a DNA microarray gene expression analysis in gut of act Gal4 UAS-toll2, elav Gal4 UAS-toll2, mef Gal4 and w^{1118} control flies. Through GeneSpring 13.0, we identified the genes that showed a statistically significant difference between control flies and flies carrying toll2 silencing and data are summarized in table 5.25. In addition, we identified ten additional genes linked to neuronal development and integrity whose expression was down-regulated more than 10-fold as compared to w^{1118} control table 5.26.

Gene Symbol	FC	GO	Gene Symbol	FC	GO
Cyp6a17	645	0016020 0005506 0009055 0016705 0040040 0055114 0043231 0020037	CG5282	20	0006508 0016805
Hex-t2	2,668	0004340 0008865 0001678 0004396 0019158 0005524 0006096 0005829	CG2781	1,104	0009922 0030497 0016021 0005575 0003843
CG1304	2,487	0004252 0006508	Fdh	791	0004022 2000169 0006066 0051903 0008542 0006069 0080164 0080007 0008270 0004552
TpI94D	813	0000785 0035093	CG8783	393	0008150 0003674 0035859
Ser6	41	0004252 0006508 0008236			

Table 5.25 Genes statistically significant

Gene Symbol	FC	GO
Tom	-48	0007423 0005515 0001736 0045746 0016360 0005737 0007219 0001708
E(spl)m4-BFM	-14	0007423 0005515 0007219 0001708 0005634 0031625
Ocho	-19	0007423 0005515 0007219
sca	-7	0008407 0005577 0046331 0005576 0097305 0016318 0007399 0007460 0048749 0008587 0016321 0004871
link	-8	0031982 0022008

Table 5.26 Downregulated genes involved in neuronal development

5.9 Efficiency of chemically inducible GAL4 drivers

To assess the efficiency and to identify the ideal working conditions of chemically inducible GAL4 drivers we crossed lines carrying ubiquitous and cellular specific (neurons, glia and smooth muscle cells) drivers with a line GAL4-GFP. Preliminary experiments identified in 100µg/ml the concentration of mifepristone required for the optimal transgene activation. In addition, the efficiency of the different drivers was quite diverse. Thus, the actin, mef and armadillo drivers seemed more effective in inducing the expression of GFP as compared to elav and repo drivers (Figure 4.27). Indeed, by comparing the GFP expression in the gut using temperature and chemically inducible drivers the mifepristone-sensitive elav and repo drivers appeared drastically less efficient than the temperature ones, whereas .

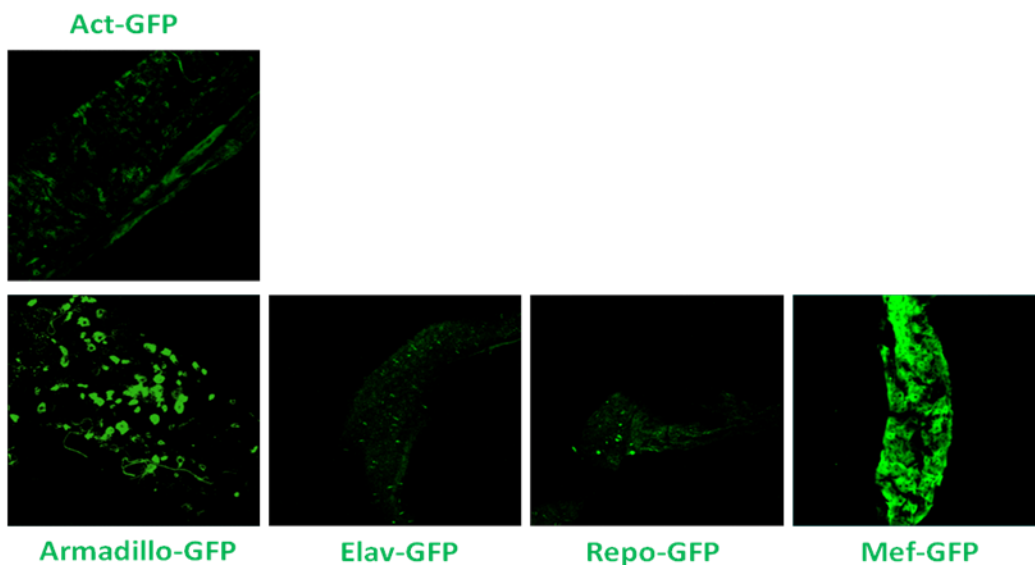


Figure 5.27 Immunofluorescent of midgut. GFP expression of GAL4 drivers in green: actin (ubiquitous), armadillo (epithelium cells), elav (neurons), repo (glia cells), mef (smooth muscle cells)

5.10 Silencing of *toll2* using the Gene Switch drivers reduced midgut neurons

To further exclude an effect of temperature on the phenotype of *toll2*-silenced flies we switched to the mifepristone-inducible system. Following 10 days of RU486 treatment the level of *toll2* silencing resulted of about 80% using the ubiquitous driver actin and also mef driver , whereas the the driver elav, inducing *toll2* silencing in neuronal cells, was

completely ineffective. Using other cellular specific driver (armadillo and repo) we observed a reduction of about 40% in toll2 mRNA level as compared to w^{1118} control, however less pronounced of the temperate sensitive drivers.

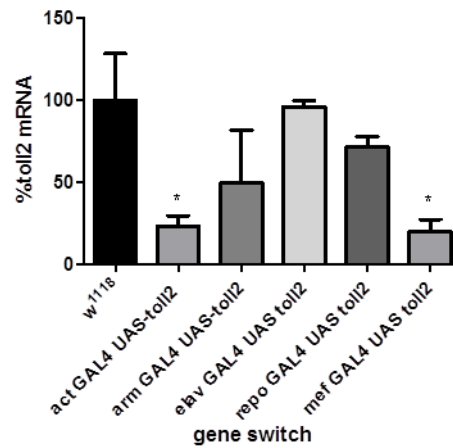


Figure 5.28 Toll2 mRNA level determined in the gut of *Drosophila* lines by qRT-PCR. (n= 3 experiments combining 20-30 gut flies). * P<0.001 versus w^{1118}

Immunofluorescent analysis of neurons in the flies midgut showed a dramatic reduction of HRP⁺ neuronal bodies in toll2 silenced flies using the ubiquitous actin and smooth muscle cells mef drivers (Figure 4.29, 4.30, 4.31). In contrast, in flies carrying toll2 silencing in neurons and glial cells there was no effect on the density of midgut neurons. Finally, in flies carrying toll2 silencing in epithelial cells a modest, although significant loss of neuronal bodies was observed, in line with the slight decrease in toll2 mRNA level.

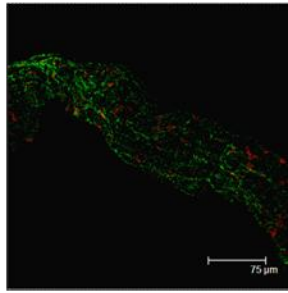


Figure 5.29 Immunofluorescence of midgut. Gut was dissected from a w^{1118} control, fixed and probed with anti-HRP antibody (neuronal bodies in red) and phalloidin (smooth muscle actin, in green). Tissues were visualized using confocal microscopy. A representative image is presented. Scale bar: 75 μm .

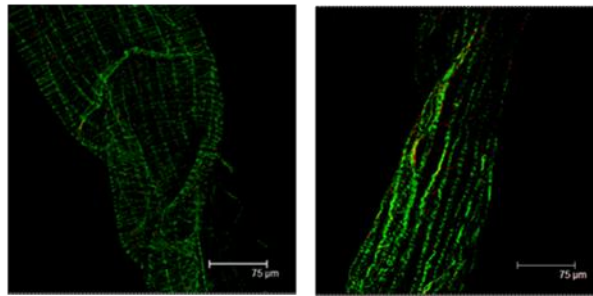


Figure 5.29 Immunofluorescence of midgut. Gut was dissected from $actGAL4 \text{ UAS } toll2$ and $mefGAL4 \text{ UAS } toll2$ exposed for 10 days to RU486. Tissues were fixed and probed with anti-HRP antibody (neuronal bodies in red) and phalloidin (smooth muscle actin, in green). Tissues were visualized using confocal microscopy. A representative image is presented. Scale bar: 75 μm .

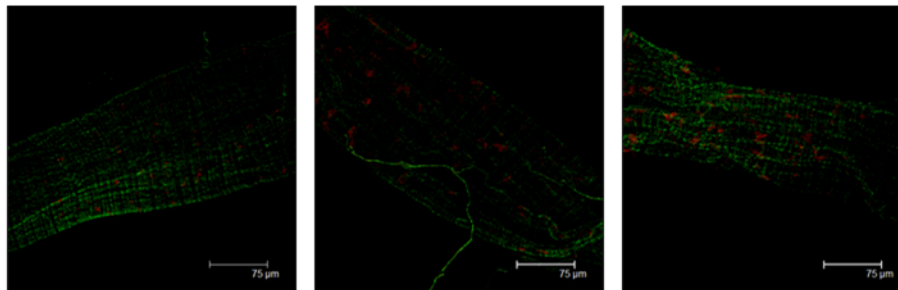


Figure 5.30 Immunofluorescence of midgut. Gut was dissected from $armGAL4 \text{ UAS } toll2$, $elavGAL4 \text{ UAS } toll2$ and $repoGAL4 \text{ UAS } toll2$ exposed for 10 days to RU486. Tissues were fixed and probed with anti-HRP antibody (neuronal bodies in red) and phalloidin (smooth muscle actin, in green). Tissues were visualized using confocal microscopy. A representative image is presented. Scale bar: 75 μm .

The direct quantification of HRP^+ neurons in the flies midgut with $toll2$ silencing using the different driver either ubiquitous and cellular specific, showed a significant reduction of neuronal bodies after 10 days of treatment with RU486 at the concentration of 100 $\mu\text{g/mL}$. (Figures 5.31).

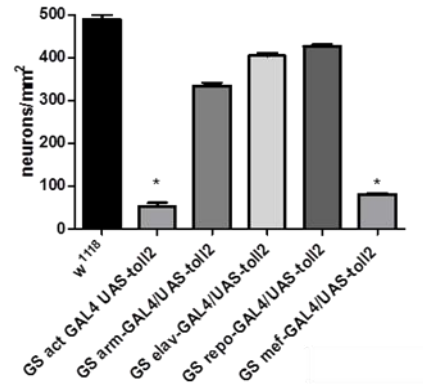


Figure 5.31: Quantification of neurons in the midgut ubiquitous and cellular specific toll2 at time t=10 (ten days after treatment with RU486) expressed as neurons/mm². * p<0.01 versus w¹¹¹⁸

To further confirm this neuronal loss we quantify the elav mRNA by real time RT-PCR. Elav is gene spreads along nerve tissue and is more precisely located at the nuclear level. As housekeeping gene we used the RP49 gene, which codes for a ribosomal protein. From real time RT-PCR data we observed a silencing of more than 50% for actin-GAL4 UAS-toll2 and mef GAL4 UAS-toll2 respect other silenced cellular specific (armadillo and repo). Also in this case elav silenced was ineffective. (figure 5.32)

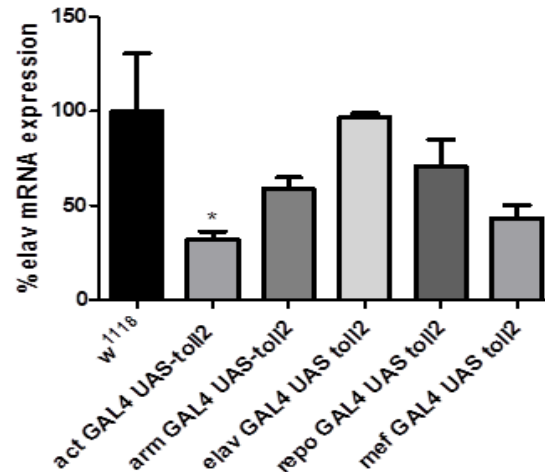


Figure 5.32 Elav mRNA level determined in the gut of Drosophila lines by qRT-PCR. (n= 3 experiments combining 20-30 gut flies). * P<0.001 versus w¹¹¹⁸

5.11 Highlight decrease survival of toll2 silenced flies following exposure to

DSS

Exposure of actin GAL4 UAS-toll2 gene switch to DSS produced different behavior than temperature silenced. Thus, contrary to what we expected, flies carrying toll2 silencing using the actin driver showed an highly decreased survival rate compared to a survival rate of w^{1118} control. (Figure 5.33).

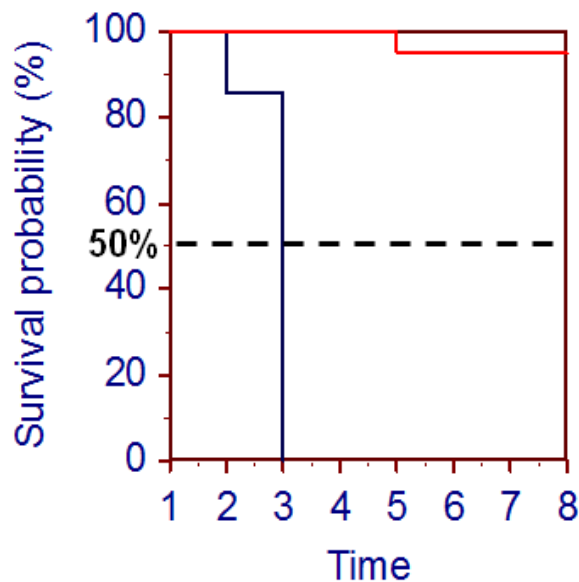


Figure 5.33 Survival curves toll2 silenced in red line control w^{1118} and in blue ubiquitous silenced act GAL4 UAS toll2

Experimental Group	Sample size	Median survival (days)
Ctrl	64	12
Act Gal4 UAS-toll2	20	2

Table 5.34 experiment data on survival curves, in the first column mutants type, in the second number of individuals, in the third median survival (days).

6 DISCUSSION

The human gastrointestinal tract houses a microbial community of about 10^{14} cells divided into more than 1000 different species, whose total genome encodes a quantity of protein that is at least 100 times higher than that of the host. The most extraordinary aspect that emerges from the latest research, is that the set of bacteria in the intestinal lumen contributes to the proper functioning of the intestine but also the welfare of the whole organism. Microorganisms can indeed integrate metabolic pathways of the host by producing enzymes that break down indigestible molecules or can directly generate soluble molecules from their metabolism regulating various functions of the host. In addition, microorganisms can interact with receptors of the innate immune expressed on various cell populations of the host triggering the synthesis and release of several soluble mediators with important effects on the physiology of the host organism. For example the activation of TLRs by molecular components retained in the intestinal microbiota modulates the immune response and maintain the integrity of the intestinal epithelial barrier.

The relevance of the signals coming from the microbiota in maintaining the well-being of the host are demonstrated by increasingly frequent detection of alterations of intestinal microbiota (dysbiosis) in individuals with diseases of the gastrointestinal tract or systemic (obesity, diabetes). Particularly in recent years several studies showed that both chronic inflammatory diseases such as IBD and functional disorders like IBS are characterized by the presence of a severe dysbiosis, although it is not yet clear how this results in the onset of gastrointestinal disorders. In inflammatory and functional gastrointestinal disorders, alterations in the structure and function of the enteric nervous system (ENS), the complex network of neurons and glia present along the whole tract, have been described.

The enteric nervous system, also called "second brain", is able to coordinate the functions of the gastrointestinal tract directly controlling the secretory activity, blood microcirculation and motility, and indirectly of inflammation and immune involving the gut, through cells of the intestinal immune system and intestinal epithelial cells (IECS). Alterations of the integrity and function of the ENS, can lead to the development of various diseases of the GI tract. In recent years, it is consolidating the hypothesis that the structural and functional integrity of the ENS depends on the type of gut microbiota present although it is still unclear what are the mechanisms through which the microbiota affects the homeostasis of the ENS. The existence of the bidirectional axis microbiota - immunity - ENS has been known by several years and seem to depend on the activation of TLRs by microbial components in order to enable both the innate immune response than that nervous to

function properly. Moreover the microflora exerts a trophic action for the intestinal tissue through the release of substances constituting the bacterial involucre or resulting from the fermentation leading to the continuous stimulation of the immune system. Thus specific Toll Like Receptor bind microbial components modulating specific bowel activities. For example, TLR2 signaling contributes to preserve the epithelial barrier and ENS integrity as well immunological responses. Changes in the composition of the microbial flora indigenous or altered signal TLR2 and TLR9 may affect the microbiota - axis TLR and then bring damage to the ENS. In the intestinal wall the different cell populations each expressing a unique set of receptors for microbial components, might generate different signals to keep intact and functional GI tract including the ENS .

The knowledge of the role of various receptors in the different cell populations would be essential for a better understanding of the pathophysiology of the GI tract and associated diseases , however, the murine models currently available are too expensive and unwieldy. For this reason it was chosen as an experimental model *Drosophila melanogaster* which is easily manipulated by the genetic point of view, with a relatively short biological cycle and with many similarities with the physiology of the human organism. In particular, the drosophila through the two pathways of innate immunity, IMD and toll, rule dialogue between host and microbiota, preserving tissue homeostasis. To analyze the role of different molecular components of innate immunity was used the technique of RNA interference (RNAi). RNAi is used to silence genes of interest and then test the impact of his absence on the physiology of the organism, in this case neurons. This system is widely used for the study of specific proteins, both in cellular systems in vitro, and in vivo in mammals, or to quickly generate transgenic flies.

In this PhD project, initially it was decided to work with a temperature-induced silencing, using driver ubiquitous and cellular-specific (neurons, glia and smooth muscle cells) activated by temperature (29°C). At first the silencing was constitutive, to see if the system UAS-GAL4 worked; then we chose an inducible silencing in adulthood because of the signal path which includes the toll is involved in the embryogenetic development and the suppression of the constitutive gene could influence the early development of the fruit fly and therefore invalidate the results.

We first tested the effectiveness of different drivers temperature inducible by GFP (green fluorescent protein) expression, than verified that toll silencing was very effective, indicating the excellent induction of various RNAi with drivers ubiquitous in line with the works in the literature. By means of the silencing of the toll2 and toll9 with constructs encoding specific

RNAi we observed in the midgut of *Drosophila* a extensive reduction in the neuronal bodies highlighted with the use of antibody anti-HRP. This antibody is widely used in the *Drosophila* field to label the neuronal surface, even if it is not known the antigen recognized. Therefore the reduction of the number of cell bodies of neurons observed in the midgut might be due to the reduction / loss of the surface antigen and not necessarily to the neuronal loss. So we performed a real time PCR analysis to quantify the specific neuronal mRNA transcripts for ELAV. This gene spreads code for a neuronal transcription factor located in nucleus. The real time RT-PCR data confirmed the IHC data supporting the loss in neuronal bodies in flies in which toll2 was silenced. We determined the impact of toll2 on flies, both in physiological conditions, by determining the survival of the insects, or exposing the transgenic flies to environmental stress that damage the intestinal mucosa. As model of mucosal damage we used DSS, already used in *Drosophila*, that seem to reproduce at least in part the mouse model with epithelial damage and subsequent epithelial regeneration. The survival of *Drosophila* exposed to DSS was significantly reduced, as also seen in previous studies. However as a result of the ubiquitous toll2 silencing, DSS exposure exacerbated colitis causing a more precocious mortality. These data seem to agree with the observation of a greater severity of colitis by DSS in mice TLR2 deficient, suggesting that signals from these receptors are needed for a balanced response to the insult. However, toll2 silencing only in muscle cells, neurons and glial, produced the opposite effect: a protection from damage and longer survival. These data seem to indicate that a loss of signals coming from specific cell populations expressing toll2, causes a different phenotype compared to a generalized silencing, which probably also includes cell populations not studied, such as epithelial cells. Furthermore, the silencing of the toll2 in neurons, glia and muscle cells is associated with a significant reduction of immunoreactivity for the HRP at the level of neuronal membranes, thus suggesting that the observed effects on survival in flies exposed to DSS could be partly attributable to the neuronal loss.

Through microarray analysis we tried to isolate genes involved in neurogenesis or neuronal survival whose expression was regulated by toll2 signaling. We have identified several genes involved in the notch pathways, implicated in the formation of nervous system as well as in neuronal differentiation and development further supporting the view that toll2-derived signals are required to support enteric neurons integrity.

Finally we have switched to UAS GAL4 system chemically inducible triggered by the molecule RU586. With this method, it is possible to induce silencing in adults already formed avoiding the temperature switch-induced stress. Using actin and mef drivers we

have obtained more than 50% silencing in the flies gut. In this case too, we observed in the midgut of *Drosophila* a wide reduction in the number of neuronal bodies highlighted with the use of antibody anti-HRP.

The fact of having confirmed for both systems a correlation between the effective silencing of the toll2 and neuronal loss, supported both immunohistochemical analysis using the antibody HRP both by PCR with the ELAV, supports the view that the innate immune system in drosophila decodes environmental generating signals essential to preserve the structural integrity of gut neurons. The loss of the signals generated by toll2 generate different effects on the survival of *Drosophila* exposed to stress according to the intestinal cell population involved, suggesting the existence of cell-specific signals axis microbiota-innate immunity-ENS. We believe that this model will be extremely useful to unravel the role of the different cellular components in generating specific signals for enteric neurons and then to identify possible therapeutic targets in patients with intestinal dysbiosis and disease.

7 BIBLIOGRAPHY

1. **Furness J. B.** The enteric nervous system and neurogastroenterology. *Nat. Rev. Gastroenterol. Hepatol.* 2012 March; 9,286–294
2. **Knowles C. H. et al.** New perspectives in the diagnosis and management of enteric neuropathies. *Nat. Rev. Gastroenterol. Hepatol.* 2013 Feb; 10,206–218
3. **Canavan C. et al.** The epidemiology of irritable bowel syndrome. *Clinical epidemiology* 2014 Feb; 6:71-80
4. **Cosnes J et al.** Epidemiology and Natural History of Inflammatory Bowel Diseases *Gastroenterol.* 2011; 140:1785–1794
5. **Ghaisas S et al.** Gut microbiome in health and disease: Linking the microbiome- gut- brain- axis and environmental factors in the pathogenesis of systemic and neurodegenerative diseases. *Elsevier journal* 2015
6. **Martínez L. and Baquero F.** Interactions among Strategies Associated with Bacterial Infection: Pathogenicity, Epidemicity, and Antibiotic Resistance. *Clinical microbiology REVIEWS* 2002 Oct , 647–679
7. **Purchiaroni F et al.** The role of intestinal microbiota and the immune system. *Eur. Rev Med Pharmacol Sci.* 2013 Feb;17(3):323-33.
8. **Dranoff G.** Cytokines in cancer pathogenesis and cancer therapy. *Nat.Cancer REVIEWS* 2004 Jan; volume 4
9. **Brun P.et al.** Toll-like receptor 2 regulates intestinal inflammation by controlling integrity of the enteric nervous system. *Gastroenterology* 2013; vol.145,no.6,pp. 1323–1333
10. **Tunis M. C. and Marshall J. C.** Toll-Like Receptor 2 as a Regulator of Oral Tolerance in the Gastrointestinal Tract. *Hindawi P. Corporation Mediators of Inflammation* 2014
11. **Anitha M. et al.** Gut microbial products regulate murine gastrointestinal motility via Toll-like Receptor 4 signaling. *Gastroenterology* 2012 Oct ; 143(4): 1006–1016.e4.
12. **Fúrie I. et al.** Epithelial toll-like receptor 9 signaling in colorectal inflammation and cancer: Clinico-pathogenic aspects. *World J Gastroenterol* 2013 July 14; 19(26): 4119-4126

13. **Gianhecchi E. and Fierabracci A.** Gene/environment interactions in the pathogenesis of autoimmunity: New insights on the role of Toll-like receptors. *Autoimmunity Reviews* 2015 Nov; Volume 14, Issue 11, Pages 971–983
14. **Ramet M.** The fruity fly *Drosophila melanogaster* unfolds the secrets of innate immunity. *Acta paediatrica Review* 2012 May; ISSN 0803-5253
15. **Apidianakis Y. and Rahme L. G.** *Drosophila melanogaster* as a model for human intestinal infection and pathology. *Disease Models & Mechanism* 2011; 4,21-30
16. **Pandei U. and Nichols C.D.** Human Disease Models in *Drosophila melanogaster* and the Role of the Fly in Therapeutic Drug Discovery. *Pharmacol Rev* 2011; 63:411–436
17. **Lamaitre B. and Alliaga I. M.** The Digestive Tract of *Drosophila melanogaster*. *Annu. Rev. Genet.* 2013; 47:377–404
18. **Robinson C.J. et al.** From Structure to Function: the Ecology of Host-Associated Microbial Communities. *Microbiology and Molecular Biology REVIEWS* 2010 Sept ; p. 453–476
19. **Broderick N. and Lemaitre B.** Gut-associated microbes of *Drosophila melanogaster*. *Gut Microbes* 2012 July/August; 3:4, 307-321
20. **Hoffmann J.A. and Reichhart J.M.** *Drosophila* innate immunity: an evolutionary perspective. *Nature immunology* 2002 Feb; volume3 no 2
21. **Ganesan S. et al.** NF- κ B/Rel Proteins and the Humoral Immune Responses of *Drosophila melanogaster*. *Curr Top Microbiol Immunol* 2011 ; 349: 25–60.
22. **Silverman N. and Maniatis T.** NF- κ B signaling pathways in mammalian and insect innate immunity. *Genes and development* 2001; 15:2321–2342
23. **Tanji T. and Tony Ip Y.** Regulators of the Toll and Imd pathways in the *Drosophila* innate immune response. *TRENDS in Immunology* 2005 April; Vol.26 No.4
24. **Lin J and Hackam D. J.** Worms, flies and four-legged friends: the applicability of biological models to the understanding of intestinal inflammatory diseases. *Disease Models & Mechanisms* 2011; 4, 447-456

25. **Amcheslavsky A. et al.** Tissue damage-induced intestinal stem cell division in *Drosophila*. *Cell Stem Cell* 2009 January 9; 4(1): 49–61.
26. **Williams M. J. et al.** The 18-wheeler mutation reveals complex antibacterial gene regulation in *Drosophila* host defense. *The EMBO Journal* 1997; Vol.16 No.20 pp.6120–6130
27. **Ooi JY et al.** The *Drosophila* Toll9 activates a constitutive antimicrobial defence., *EMBO Rep.* 2002 Jan; 3(1):82-7
28. **Brand A.H. and Perrimon N.** Targeted gene expression as a means of altering cell fates and generating dominant phenotypes. *Development* 1993, 118: 401-415